BNL-222832-2022-JAAM

Designer Nanomaterials through Programmable Assembly

J. S. Kahn

To be published in "Angewandte Chemie"

January 2022

Center for Functional Nanomaterials

Brookhaven National Laboratory

U.S. Department of Energy

USDOE Office of Science (SC), Basic Energy Sciences (BES) (SC-22)

DISCLAIMER

Title: Designer Nanomaterials through Programmable Assembly

Jason S. Kahn[1,3] and Oleg Gang[1,2,3]

[1]*Department of Chemical Engineering, Columbia University, New York, NY 10027, USA*
[2]*Department of Applied Physics and Applied Mathematics, Columbia University, New York NY 10027, USA*
[3]*Center for Functional Nanomaterials, Brookhaven National Laboratory, Upton, NY 11973, USA*

Keywords: DNA-based nanomaterials, crystal engineering, designed nanomaterials, DNA structures, nanoparticles, self-assembly

Table of Contents:

Abstract

Nanoparticles have long been recognized for their unique properties, leading to exciting potential applications across optics, electronics, magnetism, and catalysis. These specific functions often require a designed organization of particles, which includes the type of order as well as placement and relative orientation of particles of the same or different kinds. DNA nanotechnology offers the ability to introduce highly addressable bonds, tailor particle interactions, and control the geometry of bindings motifs. Here, we discuss how developments in structural DNA nanotechnology have enabled greater control over 1D, 2D, and 3D particle organizations through programmable assembly. This Review focuses on how the use of DNA binding between nanocomponents and DNA structural motifs has progressively allowed the rational formation of prescribed particle organizations. We offer insight into how DNA-based motifs and elements can be further developed to control particle organizations and how particles and DNA can be integrated into nanoscale building blocks, so-called "material voxels", to realize designer nanomaterials with desired functions

1. Introduction

Nanoscale self-assembly phenomena have driven a deep interest due to the promise of creating engineered nanomaterials that utilize unique properties of nanoparticles and the systems that can be built from them. With the desire to enable new function comes the requirement to define material organizations at the nanoscale, where systems may include diverse types of inorganic and organic nano-blocks arranged in either a periodic or non-periodic manner. Progress in understanding emergent and collective effects in multi-component, nanoscale systems and the development of new technologies based on them are impeded by a lack of a platform approaches for fabrication of designed 3D nanoscale architectures with targeted material composition. This problem is a long-standing challenge in the areas of complexly organized optical and mechanical nanoscale 3D metamaterials, quantum information systems, neuromorphic computing, and bio-hybrid devices, which require a controllable placement of different functional nano-components in space.[1] While tremendous progress has been achieved in predicting unique characteristics of novel nanomaterials, their exploration, physical realization, and applications are often limited due to constraints of conventional top-down nanofabrication approaches. These limitations include planar character of conventional nanofabrication, difficulty integrating wet-chemistry products, and coordinated placement of nanoscale components of different types into a unified architecture.

To overcome such limitations, self-assembly as a bottom-up fabrication approach has been extensively considered and investigated for the last two decades.[2] Indeed, various material classes have been used to generate ordered nanostructures through self-organization, including nanoparticles, metal-organic frameworks (MOFs), polymers, and biomolecules.[2b, 3] As nanotechnology has advanced, particularly regarding the ability to tailor nanoscale properties and interactions through materials chemistry, bottom-up assembly of materials in 1D, 2D, and 3D has seen corresponding advances in complexity, quality, and yield. Progress in nanoscale structure assembly has led to the formation of finite size clusters.[4] Yet, driven by a need to form larger scale material systems, 1D, 2D and 3D nanoparticle lattices have continued to be extensively investigated.[2b, 5] Formation of 3D nanoparticle arrays is particularly impactful, as such structures, through integration of a large number of nano-components, provide access to large-scale spatially organized nanomaterials with emergent properties. Such materials can harvest collective effects and offer a convenient format for device fabrication and processing, yet they cannot be created through traditional nanofabrication. Thus, it becomes apparent that methods for creating the desired 3D materials with designed arrangements of nanoscale blocks are needed. This ability to combine and direct diverse types of nano-blocks into desired structures would revolutionize modern nanoscale manufacturing methods and permit the creation of new types of materials for applications in energy materials,[6] information storage and electronics,[7] optics,[8] and catalysis[9].

While self-assembly typically relies on an interplay of interactions and entropic factors, as well as control over kinetic effects, complex systems may require a deliberate “delivery” of information about targeted structures. Thus, it is attractive to imagine the ability to incorporate assembly instructions into nano-blocks to govern formation of desired structures, and there are multiple mechanisms by which this user-defined information can be encoded. In a broad sense, assembly instructions can be encoded through defined interactions between nano-blocks, their shapes or binding topologies, pathway engineering through kinetic and sequential assembly protocols, or utilization of scaffolds for templating the desired structures. These additional levels of control are meant to guide entropic and enthalpic assembly conditions, favoring specific forms of interaction over others. For example, particles possessing faces or facets, such as cubic particles,

demonstrate favored interaction modes in contrast to spherical, isotropic particles.[10] By controlling binding modes, one can then favor a binding valence between material components.

DNA-based assembly methods stand out due their ability to encode information for specifying addressability of interaction, which is attractive for creating complex multicomponent systems. This opens an opportunity to program self-assembly process for the formation of targeted architectures. In the last decades, DNA has emerged as a powerful molecular assembly tool due to its stability, availability of sequence-prescribed synthesis and chemical modifications, and predictable structure. But why, despite many efforts, has DNA not yet resulted in a tailorable material fabrication platform? Starting from the early ideas of DNA organization of nanoscale materials[11] and DNA motifs for linking inorganic particles,[12] DNA-based assembly methods[5a, 13] have provided the ability to assemble nanoscale structures, including planar,[14] finite-sized DNA architectures,[5a, 14c, 15] and NP clusters[4b, 4f, 16]. However, establishing methods for forming desired complex 3D organizations of inorganic NPs that can carry a variety of functions has met a fundamental challenge: an inevitable coupling between the nature of NP (size, shape, interactions, grafted ligands) and the self-assembly process. While DNA nanotechnology has developed and led to a powerful range of methods to tailor the structure of DNA architectures in a desired way, using DNA for creating designed material systems from nanoscale objects (e.g., inorganic nanoparticles, proteins) requires strategies that account for nano-object sizes, binding modes, and other characteristics. Thus, leveraging methods for structuring purely DNA architectures with approaches suited for organizing nanoscale objects presents a unique opportunity to bring nanomaterial design methods to a qualitatively new level.

The question of creating targeted 3D materials from nano-objects is particularly important for future manufacturing since there is no technological platform despite broadly recognized needs. Although a rich diversity of 3D inorganic NP lattices,[5e, 17] and even an ability to manipulate them,[17e, 18] has been shown, the organizations are not designable and typically limited to: (i) mimicking atomic systems, (ii) mono and binary compositions, and (iii) single-scale periodicity and simple architectures. In addition to limited designability, two other requirements in forward-looking 3D assembly present significant challenges: (i) the creation of nano-architectured frameworks from diverse inorganic compounds, and (ii) digitalization of the entire fabrication process, from nanoscale assembly to macroscale material formation. Thus, a new DNA-based programmable assembly platform that incorporates wet-chemistry derived payloads over a wide range of different nanomaterial types may enable designed 3D nanostructure with control on multiple scales. While the focus of this review is fully programmable architectures using sequence-encoded Watson-Crick interactions, we also point out that in certain material applications, inter-strand binding can be carried out using covalent bonds, environment-dependent base interactions, metal-coordination bridges, electrostatic interactions, and site-specific invasion[5i, 19].

There are two broad strategies that have previously defined DNA-based assembly of materials: (a) particle assemblies based on packing or binding of DNA-functionalized particles[5e, 17a, 17b] and (b) nano-component assemblies utilizing a predefined scaffold onto which components can either bind or be grown[20]. These approaches, shown in **Figure 1**, have generally been viewed as different fields in the research community, with one focused on controlling interactions between particles and the other on creating defined, DNA-based structures. However, recent advances demonstrate that these strategies can be effectively merged, resulting in a unified DNA-based material assembly platform.[5c, 5d, 5g, 21] Particle-defined assemblies, shown in the top half of **Figure 1**, can be assembled through DNA linkages with packing arrangements that depend on the DNA shells, relative particle sizes in a mixture, and particle shapes. The same assembly strategy can be

applied to particles of different kinds, possessing optical, magnetic and catalytic functionalities, but demonstrating a formed structure that depends on the structure of DNA shells.[22] Coordination of binding partners can be altered to enable more complex organizations through changes to interaction conditions and/or particle attributes, such as aspect ratios or particle geometries. However, the particles themselves are inherently a part of the resulting structure, which stands in contrast to scaffold-defined assemblies where particles are hosted by a secondary lattice structure. These scaffolded assemblies, shown in the bottom half of **Figure 1**, utilize direct linkages between either DNA strand sets or DNA structural motifs known as DNA origami. While strands networks have been used to form 2D and 3D DNA networks, linkages between DNA origami have allowed for the development of more complex scaffolds that can also bind nanoscale objects.[5c, 5d, 21b, 23] By hosting functional materials, these structural subunits become functional nano-blocks with defined external binding characteristics and a function tied to an internally bound material, such as inorganic nanoparticles or biomolecules. Here, particles or other hosted components do not play a structural role in the assembled architecture; this significantly reduces requirements regarding their functionalization with DNA, which is beneficial for their function and ease of ready incorporation into the architecture.

The ability to couple geometrically defined DNA constructs and DNA-encoded binding between nano-components has recently allowed for the blending of these two assembly strategies by enabling addressability and topological control for the assembly of functional nano-components. This introduction of binding specificity, or 'color', to nanoscale interactions is a recent phenomenon. In this new materials paradigm, the view of a scaffold being populated through diffusion of nano-objects can be reconsidered as a self-assembly of smaller scaffold groupings pre-populated with these objects, shown as the DNA-NP framework in **Figure 1**, and organized spatially through binding color. This builds on work in the synthesis of 2D and 3D DNA crystals, most often assembled through a set of interlinked, single-stranded DNA.[15b, 15f, 24] New research has made use of various assembly pathways to organize inorganic particles and organic molecules, including enzymes, for a range of potential applications in optics, electronics, and catalysis. Additionally, where DNA-based systems were once viewed as powerful but temporary organizational tools, the structures they form can be transformed into permanent and solid-state systems through metallization and mineralization of the DNA components.[25]

The question arises, however, as material selections grow larger and desired assembly architectures grow more intricate—how best to reduce complexity of assembly processes and how to populate a nanoscale lattice with desired functional nano-blocks? What are the key factors to enable a full programmability of material formation? By breaking the mesoscopic scaffold into its component pieces, and connecting its topology with a material binding function, these questions can be tackled through rethinking the strict divide between nanoscale scaffolds and the functional nanomaterial blocks on which we seek to impose order. This review presents how researchers have made advancements to enable bottom-up assembly of particles through both particle-based effects and scaffold design to create structures of increasing complexity. From this discussion, we aim to provide an outlook using recent works to propose how novel, prescribed assemblies and addressable three-dimensional materials can be practically realized towards emerging applications that can benefit from precisely designed and organized nanomaterials.

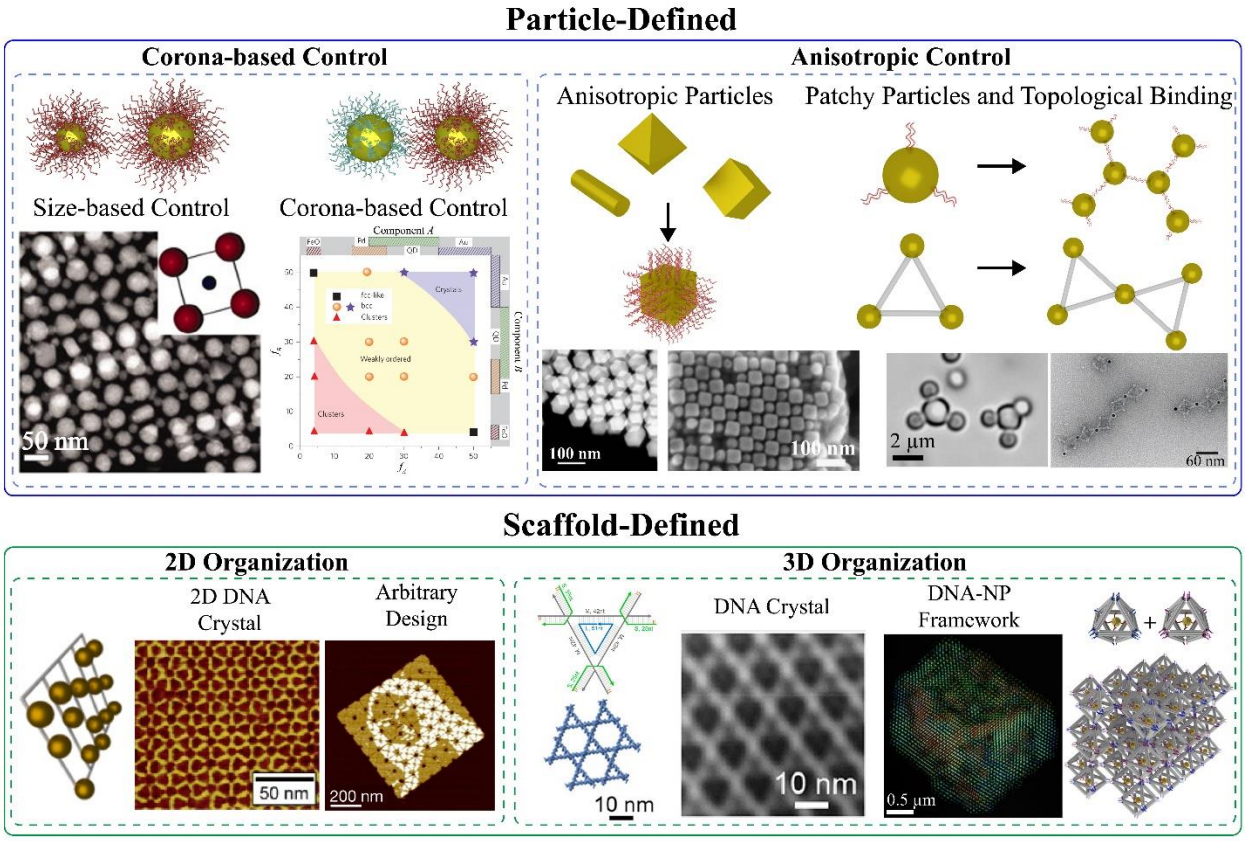

Figure 1: Organizations of particles can be induced by defining particle-particle interactions or by imparting order through specifying particle interaction with an ordered scaffold. Among particle-defined organizations (top), the development of bottom-up nanoparticle assemblies has heavily relied on defining packing interactions and energetics of binding between isotropically-functionalized particle sets.[5b, 22]Research has increasingly explored particle anisotropy through both particle shapes[10a, 26] and the engineering of inter-particle binding using a geometrically complex DNA linkers[4b, 27]. The development of scaffolds for particles placement (bottom) has generally been based on utilizing the self-assembly of DNA structures containing binding sites for particles. Until recently, such assemblies have mostly been demonstrated for one and two-dimensional organizations, including ordered DNA assemblies[20a, 20b, 28] and arbitrary organizations of components[29], or for interlinked strand networks, such as DNA crystals[15b, 24f, 30]. DNA frameworks that bind nano-components,[5c, 5d, 5g, 21b, 23] built through directly linked DNA origami, offer a unique ability to control ordering of targeted nano-components (nanoparticles and biomolecules), with prescribed binding between structural scaffold subunits and scaffold-component interactions. This figure has been adapted with permission from the following: Copyright 2021, AAAS, ref [5b]; Copyright 2021, Springer, ref [22]; Copyright 2021, Springer, ref [10a]; Copyright 2021, Springer, ref [26]; Copyright 2021, Springer, ref [27]; Copyright 2021, Springer, ref [4b]; Copyright 2021, ACS, ref [28]; Copyright 2021, Springer, ref [29]; Copyright 2021, ACS, ref [24f]; Copyright 2021, Springer, ref [5c].

2. Crystallization of DNA-coated particles

Looking towards the organization of nanoparticles, we consider how researchers have sought to create packed particle structures that serve as analogues of atomic crystal phases. While atoms have inherent, unchangeable chemistries, nanoparticles possess a functional identity that can be separated from its ability to interact with neighboring materials. Particle functionalization with polymers or ligands provides a means to control neighbor interactions, but DNA ligands demonstrate unique and unmatched control. DNA ligands offer precise control over both length and most importantly binding specificity, with hybridization between its set of 4 bases defined by Watson-Crick base-pairing. A wide range of available chemical modifications makes DNA amenable for particle functionalization while its designability also allows it to form prescribed structure. Here, we will explore methods of achieving crystallization with nanoparticles, with the aim of building binding complexity and defining particle anisotropicity to achieve different architectures through entropic and enthalpic contributions of DNA binding and particle packing.

2.1 Isotropic cores and functional coronas

The crystallization of nanoparticles can take place in any environment that energetically favors condensed phases of particles. This aggregation and packing of particles must be induced through an additional system change or energy input. There are three general methods to increase local particle concentration, including (i) evaporative removal of solvent[31], (ii) introduction of interfaces, including the air-water interface[32], and (iii) control of interaction between particles, which can be utilized to guide a formation of specific structures[11b, 33]. Particles will, given their chemical makeup and the surrounding solution environment (salts, pH), demonstrate a phase space where particular aggregations and packing arrangements predominate.

There are broad examples of polymers being used as particle modifiers to influence particle interaction, both enthalpically and entropically. DNA, however, allows further tuning of enthalpic control by supporting addressable and specific user-designed interaction through Watson-Crick base pairing between the 4 bases making up the biological polymer. In this manner, a driving enthalpic interaction in solution allows sufficient attraction between neighboring particles to enable aggregation in solution. Particle-bound DNA ligands can thus achieve a desired balance between attractive and repulsive forces by counteracting repulsion induced by steric and entropic effects of DNA chains as well as electrostatic repulsion of the polyanionic backbone.[5b, 5e, 17a, 22, 33d, 34] Moreover, the ability to control ligand length with single base resolution offers an unmatched level of homogeneity and specificity in the DNA corona design of particles.

Entropic contributions in modelling DNA-based nanoparticle organizations are more generic, concerning space-filling considerations of the corona, which in turn are related to the configurational entropy of the particle-attached polymers. DNA allows a high level of control over the balance of these forces, allowing a base-by-base design of length and binding, which directly influences enthalpic contributions while simultaneously affecting entropic influences in ssDNA/dsDNA character between particles.[35] Various formats of this DNA interaction can be designed, including direct binding between particles modified by complementary ssDNA and bridged binding through a third linker ssDNA strand present in solution with partial complementarity to the two particles, as illustrated in **Figure 2A(i, ii)**. These two formats have

been used to explore a similar range of crystal phases, but a bridged binding format allows the potential of binding modulation form a given particle set to change either spacing or crystal phase. Liu et al. used stiff DNA linkers of different lengths to demonstrate this point, achieving either hexagonal close-packed (HCP) or face-centered cubic (FCC) ordering (**Figure 2B**).[36] Topological linkers, **Figure 2A(iii)**, can be either anisotropic particles or other material binders, including structural DNA motifs. By defining different modes of binding interactions, a wider range of crystal phases can potentially be explored as compared to direct or bridged binding schemes.

A significant number of computational studies have focused on revealing the relationship between DNA-mediated interactions of nanoparticles and their assembly behavior. Much before experimental realizations, Tkachenko proposed a means to manipulate the interaction potential between colloidal particles through a combination of hybridizing and non-hybridizing strands, which promised to yield a rich phase diagram.[35a] The tuning of interparticle interactions as well as kinetic and geometric effects of assembly processes were studied extensively,[37] which provided insights into kinetics of assembly, crystallization and factors affecting the formation of lattices with specific symmetries.

Through the tuning of interparticle interactions, isotropically functionalized spherical nanoparticles have been shown to crystallize in close-packed crystal symmetries. Namely, face-centered cubic (FCC) and body-centered cubic (BCC) phases form based on a single shell type or two particle shell types, respectively.[5e, 8c, 17a] Due to the isotropic nature of crystal growth, such crystals can often have grains of competing crystal formations as there is a low barrier to formation of different habits.[33a] Recently, lattice growth from surfaces was shown as a promising approach for forming well-defined crystalline morphologies[17d]. Though only a limited number of packing organizations can be achieved using such particle systems, interesting physics can be uncovered from the resulting close-packed organizations[38] and the behavior of assemblies under osmotic pressure[39]. In both experimentally demonstrated systems and theoretically proposed assemblies,[31b, 40] the design challenge remains ligand selection for a given particle size and material composition, which in turn can affect grafting density.[33d, 41] These choices provide differing NP coverage and different energy considerations of the DNA corona, particularly in regard to modelling DNA shells comparable in size to the nanoparticle they are functionalizing.[42] Importantly, with the ability to tune particle sizes, strands length and grafting densities, a richer crystal phase space becomes accessible.

While base-pairing bindings are unique to DNA and offer unmatched control over the specificity of particle binding, it is also important to consider the contribution of solution environment to the attractive and repulsive interactions between DNA-functionalized particles, such as salt makeup and pH. DNA itself carries one negative charge per base, associated with the phosphate backbone, and thus requires salt-screening to enable stable base-paring. Magnesium presents not only a higher ionic strength than sodium at a given concentration based on its divalent nature, but has the ability to bridge and stabilize electrostatic interaction between DNA strands even without base-pairing.[33b] The ability to modify salt-screening and introduce DNA intercalators contribute to different nearest-neighbor spacing within a given crystal phase, and to switching between crystal phases, such as FCC and BCC.[33b, 43]

2.2 Binary mixtures of isotropic particles

While a wide range of crystal habits can potentially be formed through modulating the DNA functionalization of spherical particles,[5b, 33a, 33d, 41, 44] FCC and BCC phases are commonly

encountered in these systems of morphologically homogenous, spherical particles. Access to a wider phase space becomes available when increasing the complexity of particle mixtures, namely the co-crystallization of isotropic nanoparticles of different dimensions and with different levels of interaction. Such systems have been explored over a large structural phase space between particles of different materials, size, interaction strengths, and crystallization pathways using non-DNA surface ligands.[45] By manipulating the associated space-filling parameter of the system, a wide range of crystalline systems could be synthesized.[45-46] This approach can be furthered using DNA ligands, which offer a higher level of control over ligand length through single nucleotide additions and enthalpic control through Watson-Crick base pairing between particle coronas.

Given the designability of DNA coronas, topological considerations can be manipulated to explore different crystal packing and size difference limitations can be overcome by specific design of DNA lengths in respective particle coronas.[5b, 33d, 41, 47] Researchers have undertaken a thorough exploration of linker-mediated crystal phases between binary sets of particles,[5b, 33d, 41] **Figure 2C**. They demonstrated that in addition to interaction strength, access to a wider structural phase space could be achieved by modulating additional factors: (i) particle size ratio, (ii) ligand lengths as a function of particle core size (where hydrodynamic radii may be the same but particles themselves are different sizes), (iii) stoichiometric particle ratio, and (iv) ligand grafting density. Moreover, these phase changes led to associated morphological transformations in the assembled mesoscale materials through observed changes in microcrystal Wulff polyhedra.[47] Naturally, the level of interaction between two particle sets' respective DNA coronas can be modified to change both overall crystal structure as well as particle ordering within the lattice,[37b, 48] visualized with microparticles in **Figure 2D and 2E**. This demonstrates that binary superlattices are not solely formed through entropic driving forces, such as those arising from different particle sizes or anisotropic geometry, but can also be formed through enthalpic control. Understanding of these experimental systems has enabled the creation of phase diagrams using linker length, ratio of particle sizes, and stoichiometry of the particle mixture as defining parameters, which can be utilized to predict resulting structure, **Figure 2F**.[33d, 41] Such parameters can be actively modified as well, where free ssDNA can be added to a solution of crystallites that either strengthen or weaken binding between neighboring particles. For example, bond reprogramming was used to induce selective transformations between different FCC and BCC nanoparticle crystal phases.[17e]

The consideration of binary particle mixtures is more than just a conceptual argument for a greater range of crystalline order. In application, nano-objects of different materials do not either consistently possess the same size distribution nor the same surface chemistry for functionalization. Often, these chemistries are dependent on the materials being used, including linking chemistries such as thiol-linkers, amino-linkers, carboxylic acid-based linkers, biotin-streptadivin interactions, and click chemistry. Inherently, different functionalization chemistries lead to different grafting densities of linker on a particle surface, which has been demonstrated to significantly affect particle interaction and potentially mesoscale structuring.[22, 33d] Thus, determining why certain crystal phases form and the pathway to achieve a desired phase is practically important for functional applications that can include combinations of plasmonic, magnetic, catalytic, and luminescent components.

Importantly, the size of the DNA shell, which in turn imparts a characteristic shell 'softness' that influences assembly, can be tuned to overcome differences in particle shapes or sizes by engineering a hydrodynamic radius of particle plus ligand.[22] For example, a mixture of gold nanoparticles, functionalized with thiolated DNA, and quantum dots, functionalized with amino-DNA, have been arranged in a BCC lattice.[22, 44b] This result would be expected from a

two-particle gold system, but in this mixed layout the gold particle are organized in a simple cubic (SC) ordering in relation to each other. However, a critical finding in a mixed material such as this was that as corona softness, or length, was increased, structural quality increased but a concomitant compositional disorder arose (**Figure 2G**).[22] In this manner, the crystal phase and thus location of a given particle's nearest neighbor was of high certainty but the identity of that particle, whether gold nanoparticle or quantum dot, became less confident. Such insight further defines assembly rules for rationally designed assemblies, and clarifies the interplay between both specific binding and non-specific interaction in the nanoscale regime.

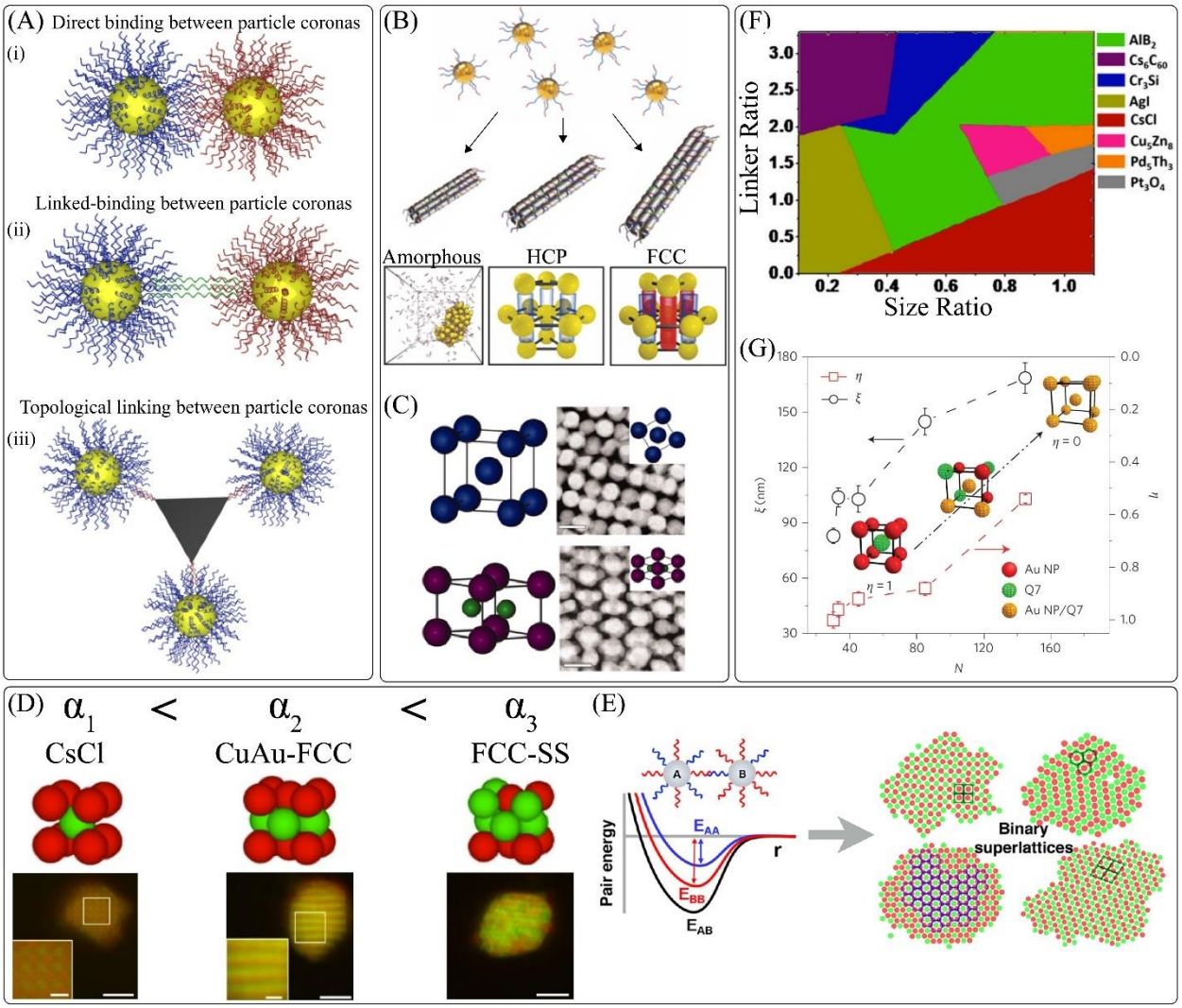

Figure 2: DNA corona design, including strength, softness, and linking ratios, induce significant differences in aggregation and crystal phases. (A) Functionalization of gold nanoparticles is most often achieved through gold-thiol linkages. Binding between neighboring particles can be accomplished through (i) complementary binding between two strands directly attached to different particle sets or (ii) through a linker strand(s) possessing partial complementarity to both particle sets. More complex arrangements of particles can be achieved through (iii) design of a topological linker. (B) Stiff, linear DNA binding constructs can be used to create nanoparticle lattices, but significant differences in organization are achieved through linkers of differing aspect

ratios.[36] (C) Various crystal phases, including BCC and Cr_3Si (top to bottom), can be synthesized through binary particle mixtures. All scale bars in TEM images are 50 nm.[5b] (D) DNA-coated microparticles demonstrate the different crystal phases achieved, and level of nearest-neighbor specificity, by modifying the level of self-interaction (α). Scale bars correspond to 2 μm and 0.5 μm in insets.[48a] (E) Similar concepts of modifying interaction strength (enthalpy) between two sets of particles can be applied to form specific binary superlattice formations in 2D.[37b] (F) Phase diagram of binary nanoparticle systems based on a forward complementary model using a genetic algorithm approach, with phases determined by varying linker ratio (grafting density on particles) and hydrodynamic radius (nanoparticle radius plus DNA corona height).[33d] (G) Plot of DNA base number vs correlation length (a measure of crystal quality, left axis, ξ) and compositional order (right axis, η).[22] This figure has been adapted with permission from the following: (B) Copyright 2021, ACS, ref [36], (C) Copyright 2021, AAAS, ref [5b], (D) Copyright 2021, Springer, ref [48a], (E) Copyright 2021, ACS, ref [37b], (F) Copyright 2021, USNAS, ref [33d], (G) Copyright 2021, Springer, ref [22].

2.3 Anisotropic cores

Though DNA can be used to overcome differences in particle size and shape, particle anisotropicity itself can be exploited to provide directed interaction at the nanoscale. As opposed to excluded volume considerations in packed isotropic particle systems (generally FCC and BCC phases), spontaneous organization of anisotropic particles is governed by an entropy maximization achieved through maximized contact area.[10, 11b] Through organization of the flat facets on a polyhedral object, preferential three-dimensional alignments can be supported. Spherical particles inherently do not contain directionality in their interactions, and thus resulting lattice constructs are completely based on modifying enthalpic and entropic tradeoffs of an engineered corona. Based on an additional entropic consideration, anisotropic nanoparticles synthesized in a variety of different shapes including cubic, octahedral, and bipyramidal structures, provide a further means of controlling phase formation. Anisotropic particle cores allow access to a form of directional interaction where defined particle faces facilitate organization along specified growth directions and thus offers a means of accessing further crystal habits inaccessible by isotropic particle packing.[10a, 49]

Organization through flat facets, rather than an isotropic curved surface, is supported by a number of mechanisms that lower the interaction barrier in these arrangements. In particular, these include the denser arrangement of interactions along the face of the facet and the reduced stress of organizing along a non-curved surface.[10, 11b] The power of this strategy has been demonstrated theoretically and experimentally for both microscale and nanoscale particles, shown in **Figure 3A-C**.[10b, 11b, 33c, 49d, 50] One of the intrinsic challenges is the ability to create specifically defined anisotropic building blocks of pre-determined shapes with sufficiently low polydispersity to achieve a specific structural arrangement.[10a, 26, 49a] Additionally, the challenges in controlling resulting phases becomes even greater when the nanoscale effects of ligand density can significantly modulate the effective interactions and packing.[49c, 51] As mentioned, where the desired structure is either an FCC or BCC lattice with alternating particle types, the coronas can be engineered to mimic an isotropic particle and mask anisotropic faces.[10a, 47] Where different resulting crystal organizations are desired, recent work has shown the potential to achieve complex crystalline organizations, including clathrate crystals.[52] Such clathrate organization is achieved

through the tailoring of bipyramidal particles, **Figure 3A**, yielding various assembly subtypes based on changing parameters such as DNA grafting length, **Figure 3A(ii)**.

Combinations of particle geometries naturally will have a tendency to phase separate given entropic packing considerations,[53] yet it has been demonstrated co-assembly can be favored through tailored interaction. For example, functionalized spheres in combination with either cubes or octahedra possessing complementary ssDNA yield various assemblies of different crystalline flavors by directing interaction between the spherical particles, as shown in **Figure 3B**.[26] In this manner, complementary-binding DNA is used to overcome the tendency for phase separation of differently-shaped particles. While such systems make use of directionality in anisotropic binding, anisotropic particles themselves, as mentioned, display novel behavior with respect to surface density of DNA and the resulting functional corona. Fang et al. demonstrated that resulting ssDNA density for a nanocube is based on DNA length, where shorter strands (16 bases) favor face functionalization and longer strands (86 bases) the edges/vertices.[51] This range of interactions allowed not only the formation of a range of crystal phases from one type of anisotropic particle, including simple cubic, body center tetragonal, and body-centered cubic, but also allowed a breaking of orientational symmetry within a unit cell through a so-called 'zig-zag' pattern, **Figure 3C**. A related phenomenon in DNA binding was achieved through decorating an anisotropic particle rod with DNA of different lengths, where a preferential mesoscale linear assembly of nanorods was achieved using longer DNA lengths.[54] This insight into particle functionalization introduces the concept of further controlling where ligand binding takes place on a particle through patchy particle synthesis.

2.4 Patchy particles

Anisotropy is not solely a function of particle shape but can be induced through the introduction of interaction 'patches' on a spherical surface. This artificial introduction of 'facets' has a similar overall effect on assembly as particle anisotropy—to guide valence and coordination of neighboring interactions. However, rather than purely being a consequence of entropic facet alignment, maximized binding enthalpy serves as the driving force within this context. This idea is powerful and attractive due to the ability to specifically tailor binding direction and valence on isotropic particles, and it has been investigated theoretically to understand possible phase diagrams and design approaches.[55] Practical realizations of this approach towards actually assembly of mesoscopic materials are nascent, yet more recent research has achieved patchy nanoparticle synthesis that has only previously been demonstrated at the microscale**, Figure 3D-F**.[27, 56]

Janus particles provide some of the earliest examples of patchy interactions, particularly considering microparticle organization.[57] Their synthesis is most commonly achieved by functionalizing a portion of a microparticle by quarantining particle surface area through surface-binding and conducting either vapor or solution-based reactions on the free surface. While most often utilized in microscale particle systems, such as in copolymer strings possessing 2D particle patchiness,[27] this Janus particle technique has also been demonstrated at the nanoscale, showing specific cluster formation as opposed to larger scale assemblies.[4a] Other methods for more complex patchy arrangements,[58] some using DNA,[27, 59] have also been demonstrated on microparticles, showing the potential to form assemblies from prescribed bonding.[57, 60] This ability to create patchy microparticles, as well as particle clusters, has recently been utilized to create a colloidal diamond crystal.[61]

The apparent difference in progress concerning patchy particle organization using microscale vs nanoscale nano-blocks is explained by the addition of arranged binding sites to nanoparticles being a far greater challenge than their analogous microscale counterparts. Bulk material strategies, such as depositions and evaporative coatings, do not directly transfer to the nanoscale regime, and only recently have methods specifically been developed for nanoscale systems, such as DNA origami 'stamps'.[62] 2D stamping onto a nanoparticle has been demonstrated,[62a] as shown in **Figure 3D**, while only very recently 3D stamping has taken place. Applying this concept of molecular 'stamping' onto 3D nanoparticles is considerably more difficult to achieve than 2D systems due to more complex topological considerations. Full framing of a nanoparticle is needed, although it is also possible to form a particle within a frame itself. In the case of particle formation, a polymer-based particle, rather than being directly 'imprinted' in a traditional sense, was formed with preset binding sites inside a DNA scaffold.[63] In demonstrating imprinting onto metal nanoparticles, Shen et al. utilized a DNA origami 'clamp' to pattern ssDNA onto a gold nanorod.[62c] This methodology has recently been expanded for the transfer of three-dimensional patches onto an approximately 13 nm nanoparticle sphere using DNA nanocages, where the nanocage presents thiolated ssDNA towards its interior, covalently binding to the nanoparticle surface in predetermined arrangements.[64] As opposed to the covalent linking of binding sequences, Yan et al. used DNA strand transfer to spatially pattern a nanoparticle using a wireframe DNA construct.[65] Nanoparticles were patterned with one or several kinds sequences of DNA strands using a tetrahedron frame, and these patchy particles were further used to assemble designed clusters of nano-components, **Figure 3E.**

Specific coating of nanoparticle surfaces can also be approached by taking advantage of different polymer conformations in selected solvents to control particle patchiness, which was demonstrated through the use of polystyrene as a particle capping agent for nanocubes. In this case, reducing solvent 'quality' through addition of water to dimethylformamide (DMF) led to reorganization of the polystyrene to particle edges, and thus allowed for an etching of the free nanocube surface into a spherical structure with three defined patches.[62b] New research has shed light on how to expand regioselective encoding at the nanoscale by controlling interfacial tension between nanoparticle, solvent, and polymer through surface blocking to produce different particle shapes and encoded binding modes, **Figure 3F**.[66] While all of these novel strategies discussed do demonstrate significant progress in developing new concepts for patchy functionalization at the nanoscale, the implementation of these patchy systems remains quite challenging. Particularly, the yields and fidelity of patchy structuring necessary to assemble materials into mesoscale lattice architectures must be further developed.[62a, 67]

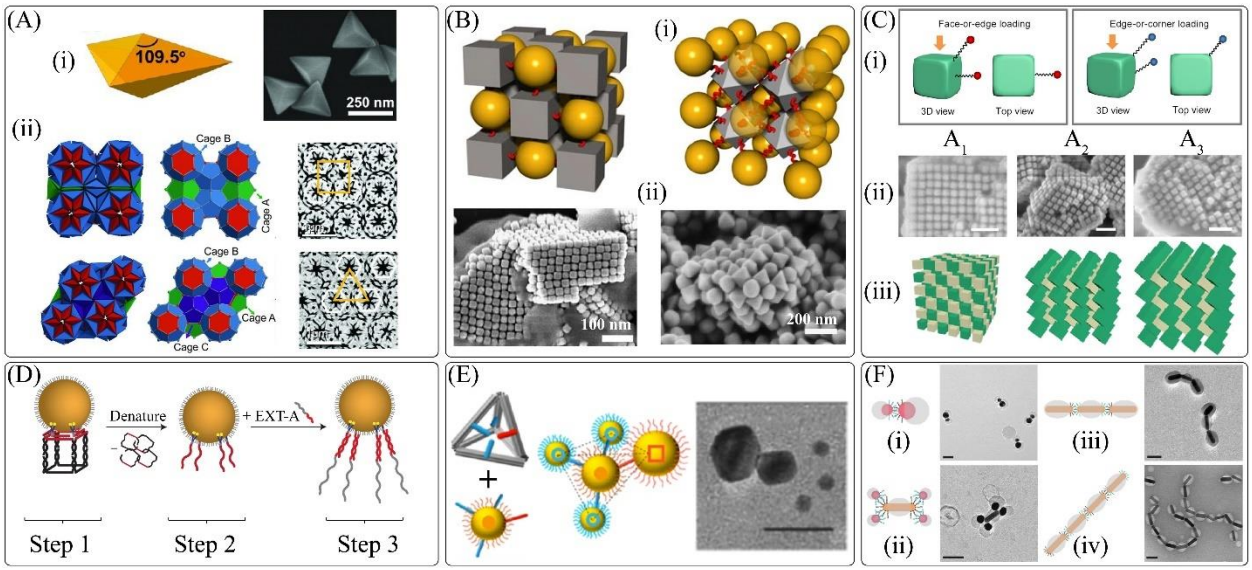

Figure 3: Anisotropic particles and resulting DNA corona anisotropicity (A-C), as well as controlled DNA binding in designated 'patches' (D-F), can lead to complex, mixed phases through directed binding. (A) (i) Schematic and SEM image of bipyramidal structures used to form clathrate crystal phases. (ii) Different clathrate orderings form depending on the facets or vertices used to conduct ordering.[52] (B) Anisotropic particle sets can be utilized as homocrystal components, or as a mixture of shapes in a heterogenous crystal. The resulting crystals from these different shapes are produced through a consideration of binding partner size and geometric configurations, with (i) schematic and (ii) SEM images of speres with cubes (left) and octahedra (right) showing the varied crystal phases.[26] (C) (i) Definition of face-or-edge and edge-or-corner loading of DNA (ii) SEM images showing various structural configurations (SC, BCT, BCC) of crystallized nanoparticle cubes. Scale bars, 200 nm. (iii) 3D models associated with each of the structural configurations.[51] (D) Patchy particle functionalization on nanoparticles through imprinting of single-stranded DNA with an engineered, reusable DNA cage nanostructure.[62a] (E) A DNA origami nanocage can be used to functionalize a nanoparticle with a defined coordination of binding ssDNA, which may possess different binding specifities. This imparts control over binding topology as well as binding partner, enabling controlled organization of different materials. Scale bar corresponds to 25 nm.[65] (F) By tuning the interfacial free energies between nanoparticles, solvent, and a diblock copolymer, varying surface areas of gold nanoparticles could be functionalized with binding ssDNA. Resulting assemblies of particle sphere and rods included both discrete (i-iii) and periodic structures (iv).[66] This figure has been adapted with permission from the following: (A) Copyright 2021, AAAS, ref [52] (B) Copyright 2021, Springer, ref [26] (C) Copyright 2021, Springer, ref [51], (D) Copyright 2021, Springer, ref [62a], (E) Copyright 2021, ACS, ref [65], (F) Copyright 2021, Springer, ref [66].

3. Imparting order through scaffolds

Accessing crystalline order through particle packing entails an inherently complex set of interactions that can be difficult to engineer in a predetermined manner. Three-dimensional scaffold frameworks, however, offer a potential alternative path towards imparting structure on particle systems without navigating the same delicate enthalpy-entropy balance as in packed

particle systems. Various methods exist outside of DNA nanotechnology that enable formation of structural scaffolds, including block copolymer organizations, backfilling interstitial space in packed microparticles, and a 'hub and spoke' design model of organic ligands and metal ion coordination centers, specifically MOFs. By incorporating functional materials of interest into such scaffolds, it is possible to access organizations not possible through direct packing.

Such systems, however, do possess inherent limitations as scaffolding for nanomaterials assembly. Block-copolymers demonstrate self-organization due to designed balances of hydrophilic and hydrophobic parameters. As such, the order is not specifically crystalline, but does offer a level of control over spacing parameters and allows for controlled etching/functionalization of surfaces for particle attachment.[8b, 68] As mentioned, three-dimensional networks can also be produced using interstitial filling of packed microparticle systems.[69] However, these packing arrangements are often quite limited, and most often the resulting interstitial framework yields an inverse opal lattice which can be used for materials depositions and growth.[70] More versatile are MOF lattices, where the use of organic ligands in combination with multivalent binding centers allows for the deliberate synthesis of 3D materials with desired crystalline characteristics. Tailorability in pore design[71] has enabled applications involving functional guests with applications in molecular storage, sensing, and catalysis.[72] While examples exist of particle incorporation and/or growth of nanoparticles inside the crystalline framework,[71c, 73] the vast majority involve the smallest classes of nanoparticles (<5 nm) and yield incompletely-filled networks.

In addition to these drawbacks, lacking in all of these approaches is the ability to specifically anchor nano-components at selected sites, thus relegating organization to particle growth or what can be achieved through diffusion into a porous network. In contrast, DNA scaffolds can be built from structural monomers, such as DNA tiles or origami, that offer (i) a structural tailorability not found in non-biological chemistries, (ii) the ability to associate nano-components with designated monomers before lattice synthesis through specific binding, and (iii) the unique ability to create 'colored' (uniquely addressable) binding specificities, where binding modes can be defined with regards to coordination, valence, and specificity. Recent works have brought DNA nanotechnology into the field of particle scaffold synthesis, and offer newfound control over binding coordination and specificity. Notably, the evolution from design of topological linkers between nanoparticles, **Figure 4A**, to the full synthesis of directly-bound DNA frameworks with internally bound materials, **Figure 5A**, marks an important conceptual change in design that guides future work.

3.1 DNA origami frames and topological linkers

DNA structural nanotechnology has seen rapid progress in producing a wide range of structure at the nanoscale, most notably through DNA origami, and opens up a new ability to define particle binding 'patchiness'. In a similar manner to which spherical particles can be co-crystallized with cubic particles to create directional binding,[26] **Figure 3B**, origami of defined topologies can be synthesized as topological linkers between spherical particles. Three-dimensional DNA origami has used to construct 1D, 2D, and 3D assemblies,[4b, 21b, 23] using designed DNA architectures as a topological particle binder, as shown in **Figure 4A(i)**.

In using origami as a topological linker between particles, one can define the binding coordination through steric limitation and entropic energy costs of binding a large, defined structure over a particle surface.[21b] The defined DNA frame geometry allows for control of

structures in different dimensions,[4b] as shown in **Figure 4B**. It is clear that the ability to control coordination, as well as binding valence, between particles has a powerful effect on the resulting macroscale organization. Modelling of these systems demonstrates that different topologies produce different desired crystal classes, and these topologies can then be produced through origami design. For example, a particle FCC lattice can be achieved through use of octahedral origami linkers, **Figure 4C,** while tetragonal lattices can be synthesized using cubic origami.[21b]

The concept of using a DNA frame to 'imprint' a binding coordination for patchy particles also suggests the ability to bind a nanoparticle within an exterior frame. In this manner, the DNA frame attachment is not a temporary binding state to enable further organization of the particle, but rather a permanent state in which the material properties of the bound material may be used while its binding definitions are encoded externally. This is a fundamental change from previous systems using discrete DNA origami as nanoscale scaffolding tools, such as chiral particle assemblies.[8a, 8d] For example, a DNA frame method has been used to organize 1D and 2D assemblies, such as the use of DNA origami constructs to create particle 'nanoflowers' that impart 2D control over binding properties.[74]

In further expanding this frame methodology by creating DNA origami frameworks where both internal and external binding can be designed, the organizational potential of DNA material scaffolds begins to take greater shape. Carrying through an earlier concept of using topologically-defined particle linkers, the origami can be engineered to possess internally-oriented particle-binding sequences, **Figure 4A(ii)**. This setup enables difficult-to-assemble crystal classes that have not been successfully synthesized using nanoparticles. Notably, a diamond lattice can be formed by tetrahedra possessing an internally-linked particle and capable of binding 4 external particles, as shown in **Figure 4D**.[23] This work represented the first synthesis of a diamond particle lattice, achieved by the ability to tailor structure at the nanoscale.

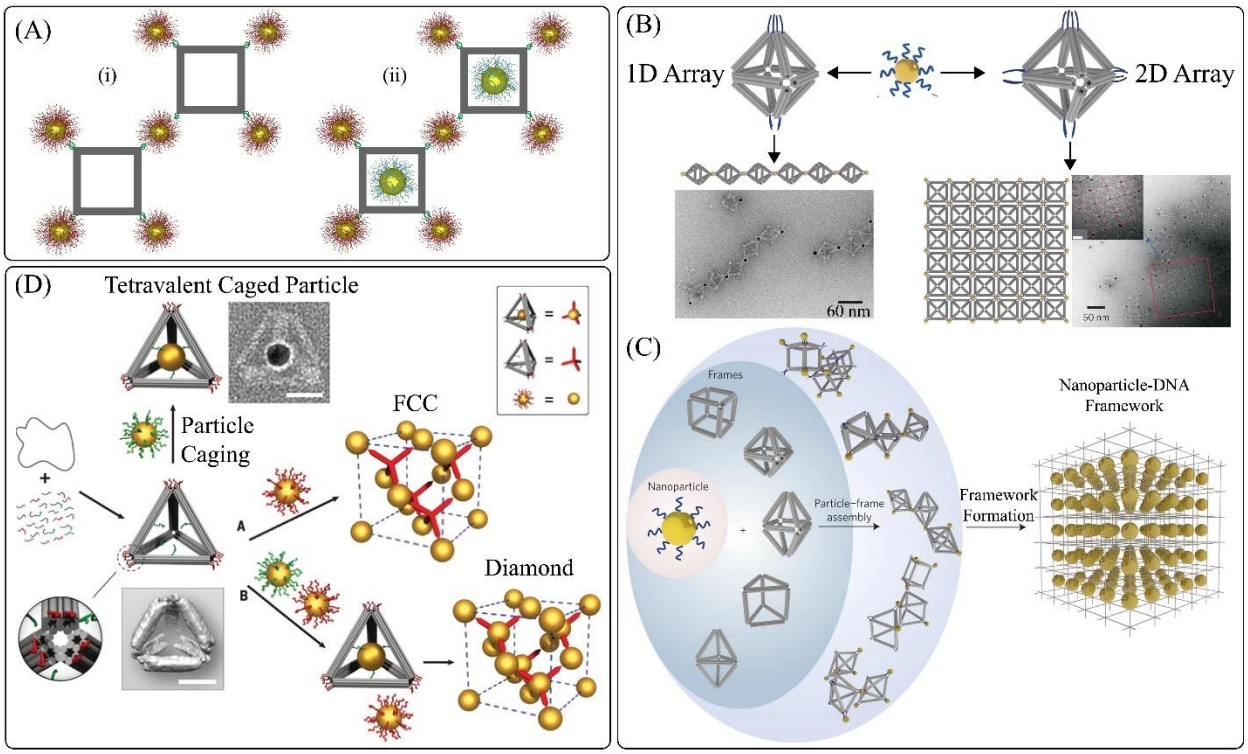

Figure 4: DNA origami can provide prescribed, complex linker topologies between nanoparticles to gain control over directional binding interactions. (A) Origami can be utilized (i) solely as topological linkers, or as (ii) dual-function linkers, possessing the ability to define binding between particles and internally bind materials. (B) An analogy to patchy particle binding can be achieved by specifically engineering topological DNA origami-linking structures, whereby a particle can only bind a specific number of partners in an energetically favorable spatial organization.[4b] (C) The extension of topological linking in 3D space offers access to crystal synthesis using a wide range of different linkers, which in turn leads to different crystal phases.[21b] (D) Combining topological linkers with binding sites in the internal volume of the linker enabled the first nanoparticle-based diamond lattice.[23] This figure has been adapted with permission from the following: (B) Copyright 2021, Springer, ref [4b], (C) Copyright 2021, Springer, ref [21b], (D) Copyright 2021, AAAS, ref [23].

3.2 Structural DNA frameworks

The capability to produce scaffold networks from predesigned geometries and binding parameters is most clearly seen through the use of structural DNA nanotechnology. This method has been particularly powerful in organizing two-dimensional networks, as the interactions of ssDNA sets allows crossover networks of repeating structure as well as the arrangement of simple structures, such as tensegrity triangles.[24a, 24b, 75] More complex structure created through DNA origami can also be controlled through arrangements of binding strands to create all DNA scaffolds that can internally bind materials, shown in **Figure 5A**.

The simplest variation of a DNA crystal is one formed by an interlinking set of two ssDNA. By utilizing sequence symmetry, both sheets and periodic patterns were formed.[24a, 24b, 75] While this yields a dense network of strands, 2D crystals utilizing specifically-defined DNA topologies can also be synthesized.[24a, 28, 75a, 76] A defined 2D topology has binding strands on the exterior of the designed shape, and thus possesses a predefined binding valence and coordination. A wide variety of geometries have been used, particularly hexagonal[75a, 77] and six-sided star-shaped DNA structures.[28] These patterns have been utilized as templates for both thermal evaporative coatings and the attachment of nanoparticles.[76]

This concept can be expanded to include coordination and binding in three dimensions. In doing this, local 3D structure can be applied into large scale, 3D organization. Similar to the 2D assemblies, 3D structure can be achieved either by using an interacting set of ssDNA, such that a group of strands organize through thermal annealing to form interlinked and networked tensegrity triangles,[5a, 15b, 24c, 24f] or by the use of pre-defined topologies formed from DNA origami. Seeman and coworkers have demonstrated a high-level of control over tensegrity-triangle networks formed through solution annealing of ssDNA, yielding high quality DNA crystals, **Figure 5B**. Recent work has demonstrated the ability to capture both particles and proteins within this crystalline network.[24f]

The formation of 3D crystalline DNA scaffolds has also been demonstrated using pre-defined DNA origami. Previously, as shown in **Figure 4**, the resulting crystal phase still required nodal binding through isotropic, spherical particles. More recent research has expanded on the use of DNA origami as designable structural monomers in the formation of a 3D scaffold through direct interactions between these structures, **Figure 5A(i)**. For example, Liedl and coworkers produced a networked, three-dimensional DNA scaffold through stacking interactions between

preformed origami, as seen in Figure **5C(i)**.[5d] This design could include binding sites for nanoparticles, as seen in **Figure 5C(ii)**.

As opposed to this base-stacking interaction, Gang and coworkers utilized direct hybridization at the vertices of a DNA octahedron, thermally annealed into a 3D network. In this manner, the interior origami volume can be used to incorporate different classes of nano-components. These structural monomers are termed 'material voxels' to encompass their ability to define a generic material's binding coordination and valence in 3D space, as seen in **Figure 5D(i)**. By alternating nanoparticle 'on' and 'off' positions, SC and FCC particle crystals could be formed, **Figure 5D(ii)**. Through incorporation of biomolecules, such as enzymes, and quantum dots, the versatility to use such material voxels in catalytic and optical applications was demonstrated. Additional recent works have demonstrated the ability to capture and pattern enzymes in a 3D lattice[5c, 24f] and to maintain enzymatic activity inside this architecture. Such novel organization provides the ability to couple catalytic reactions to an imposed ordering, enabling exploration of synergistic organizations in 3D space. In this manner, material functionality and organization at the nanoscale, which have always been intimately associated, can finally be decoupled based on a desired application. Moreover, the ability to utilize covalent bonds between DNA frames allows for permanent crosslinking of formed architectures.[19a]

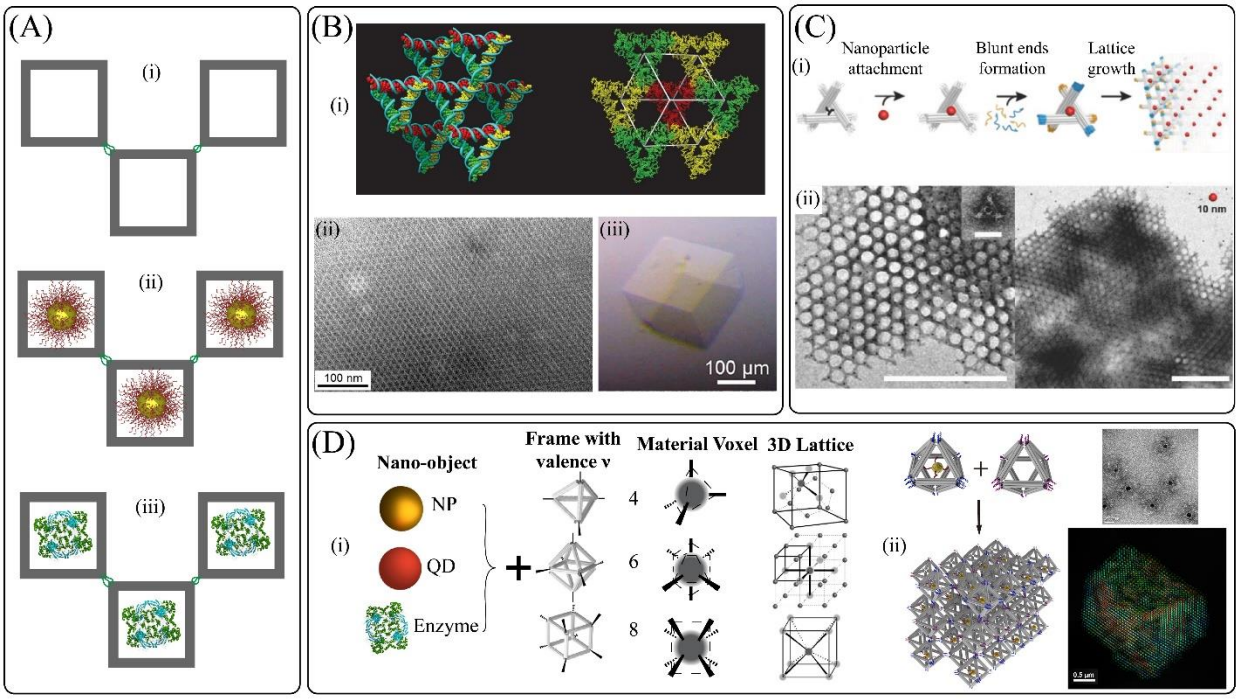

Figure 5: DNA structural frameworks can be synthesized through design of direct interactions between either ssDNA sets or pre-defined DNA topologies. (A) DNA crystals can exist as (i) all-DNA frameworks, or (ii) possess binding sites for nanoparticles or other classes of functional materials, such as (iii) enzymes and catalytic biomolecules. (B) Networking of ssDNA annealed in solution can form a 3D DNA crystal through tensegrity triangle formation.[15b, 24f] (i) 3D model showing three independent lattice directions, represented by different colors (left) with an outline of the rhombohedral cavity formed through this organization (right). (ii) SEM imaging reveals long-range order, with (iii) optical imaging confirming the resulting DNA crystal. (C) (i) A

preformed DNA origami tensegrity triangle can self-assemble in 3D space using base-stacking interaction, as opposed to sequence hybridization. (ii) TEM imaging of lattices with the capability of incorporating gold nanoparticles (10 nm in left image, 20 nm in right image).[5d] (D) (i) The synthesis of material voxels, controlling an internally-placed material's binding coordination and valence, can be used to produce different crystal phases. (ii) Origami sets can be designed to encode internal material binding, producing an FCC phase with respect to alternating particle placement from a SC origami scaffold. The lower right image displays a Cryo-STEM reconstruction of single origami with multiple streptavidin proteins bound internally.[5c] This figure has been adapted with permission from the following: (B) Copyright 2021, ref [15b]; Copyright 2021, ACS, ref [24f] (C) Copyright 2021, Wiley-VCH, ref [5d], (D) Copyright 2021, Springer, ref [5c].

3.3 'Colored' bonds for programmable assembly

A transformative view of programming a three-dimensional materials assembly requires stepping away from the convention of an either/or methodology regarding particle vs scaffold assemblies. Through addition of binding and interaction specificity into 3D lattice formation, mesoscopic structure can now be formed with complexities not possible only a few years ago. In this manner, these two views converge by having to integrate desired local interaction and coordination with a global view of lattice organization. The material voxel, described in **Figure 5D**, can be viewed as a single DNA frame and material-binding unit with a user-described coordination and valence that furthers define the overall DNA scaffold structuring a desired lattice.

"Chromatic" ("colored") binding represents the addition of specificity into a nano-object's binding coordination and valence, and this chromatic bond can be encoded through one or multiple ("polychromatic") strands[4g, 5g, 21a]. In this manner, it is largely different than isotropic particle systems coated with specific DNA sequences and presents another dimension in DNA-framed particle systems. Though sets of different DNA-functionalized particles can be grouped to change their organization in a given crystal lattice based on binding strengths and geometric packing, chromatic binding is a dramatic enabling-property because it allows specificity, and thus anisotropy, in binding partners at each binding site of a patchy binding network.

Through addition of specificity, we can begin to see how richer, more versatile organizations can be achieved. **Figure 6A** provides an example of how specific, or 'colored', binding can be viewed in the context of material binding along with material 'class' (in this case, containing a particle vs an empty space)[5g]. In this manner, a rich set of particle options can be produced and mixed, with resulting periodic and non-periodic structure arising from different particle subsets (**Figure 6B**). This coloring of interaction type overcomes fundamental limitations in the synthesis of 3D structure based on manipulating an enthalpy and entropy balance solely through topological packing, and more resembles 3D printing at the nanoscale.

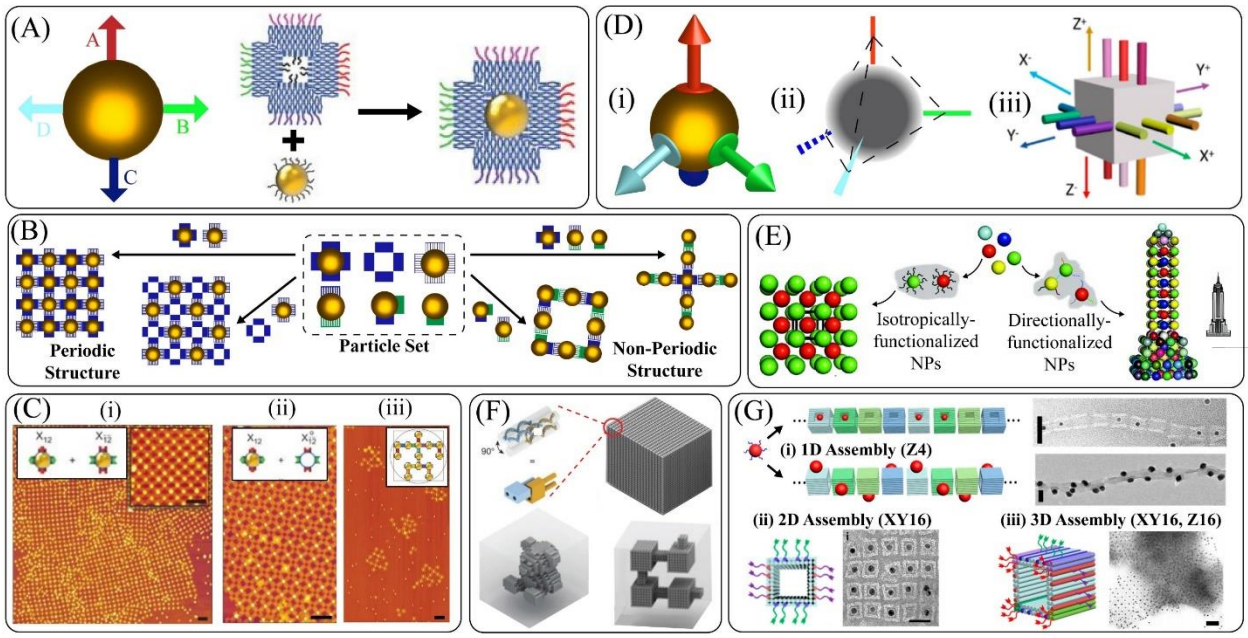

Figure 6: The coupling of binding specificity, or 'color', with defined coordination and valence allows for the synthesis of non-periodic structure, periodic structure, and complex periodic structures for the synthesis of mesoscopic materials. (A) The introduction of a 2D-DNA frame around an isotropic particle provides both a defined binding partner number and type through specific DNA binding.[5g] (B) A set of particles presenting different binding coordination and specificities can be mixed in different variations to produce both prescribed periodic or non-periodic structure. (C) AFM images presenting realized periodic (i and ii) and non-periodic (iii) structure from 2D-DNA origami frames with control over binding coordination and specificity.[5g] (D) (i) Application of colored binding in 3D space to a nanoparticle surface, (ii) a schematic outline of a frame needed to achieve a tetrameric binding coordination, and (iii) the use of multiple binding specificities/colors within a single binding interaction.[21a] (E) Binding color can be introduced isotropically or directionally, with resulting effects on the mesoscopic growth of periodic or discrete structures.[67] (F) DNA bricks possess fully-defined binding and 3D control in a limited scale system, providing the ability to etch interior spaces inside a dense DNA cuboid.[78] (G) Binding interactions between frames can contain multiple bonds with a specific directionality in color layout. (i) 1D assemblies of DNA nano-chambers, consisting of 4 bonds in the z-direction, can be stacked consecutively with or without a rotational component to the color binding scheme. (ii) 2D and (iii) 3D assemblies can be achieved by changing the strength, number, and layout of the binding strands on the nano-chambers.[21a] This figure has been adapted with permission from the following: (A,C) Copyright 2021, Springer, ref [5g], (D,G) Copyright 2021, ACS, ref [21a], (E) Copyright 2021, APS, ref [67], (F) Copyright 2021, Springer, ref [78].

Figure 6C shows the realization of designated structure through chromatic, patchy interactions. Gang and coworkers used a two-dimensional, planar hollow square origami structure, illustrated in **Figure 6A**, to internally bind a spherical particle and then confine it to a "colored" valence of four with a planar, square binding coordination.[5g] This integration of nanoparticle with origami in a building block with complexly prescribed colored interactions opens possibilities for modular design. For example, such a platform allows the assembly of what may appear to be two

equivalent, 2D scaffold sheets (**Figure 6C(i) and (ii)**), but in fact are structurally identical scaffolds with differing particle binding specificities. Through mixing of a different elements of a colored set, prescribed non-periodic structure can be achieved (**Figure 6B(iii)**). The relationship between assembly encoding of desired structures and the design of colored bonds, their strengths and stoichiometry of components was investigated in detail.[5g]

Chromatic binding can be applied more generically towards interactions in 3D space, as viewed through the lens of a nanoparticle demonstrating chromatic, tetrameric binding in **Figure 6D**. An idealized view is represented in (i) while a sketch of a potential material frame to achieve this patchy binding is shown in (ii). The realization of 2D-encoded binding organization provides further support for the promise of 3D encoded chromatic binding structures, as discussed in theoretical works considering chromatic binding capabilities on patchy particles through DNA binding specificity.[5g, 67, 79] While sets of isotropically-functionalized nanoparticles can yield designated periodic structure, as discussed in the 2D case, directional, chromatic particle interactions in 3D space provide the ability to fully encode mesoscale object structure, **Figure 6E**.[67]

These methods consider the particle and its associated DNA as a nano-block capable of organization. In the realm of purely DNA-based structures, a dense volumetric scaffolds, consisting of 10,000 structurally identical, yet sequence-specific, DNA 'bricks' with about 20,000 voxels, has been constructed.[78, 80] This resulting cuboid structure can then be synthesized with designed 3D cavities in its interior, confirmed by microscopy and DNA sequencing. As the space is entirely addressable, complex cavities could be formed, as seen **Figure 6F**. It is important to note that this technique created a negative-space structure, and required a subtractive process from a dense structure set to achieve the final design. Though this method does provide complete addressability and high resolution, it has limitations when attempting to apply this assembly concept to materials. As powerful nanoscale assembly methods move from DNA-only structures to nanomaterials, methods to structure nano-objects with such exquisite levels of control in 3D need to be established. We stress that the discussed DNA-brick methodology cannot be simply "copied" for nano-objects.

While the DNA-brick method powerfully shows the ability to encode specificity at the nanoscale using DNA, the use of chromatic binding in conjunction with defined coordination and valence can be used to create structure from a minimal set of DNA or nano-object components. In this truly bottom-up method, a system can be optimized to include a minimal, but sufficient, amount of complexity to provide a desired periodic or non-periodic mesoscale architecture. A system does not have to be fully defined at every material position, and significantly fewer unique monomer structures are needed to synthesize a specific lattice layout or crystal group than required spatial positions. In this manner, large-scale organizations can practically be formed. Tikhomirov et al. utilized a 2D hierarchical, fractal assembly method to create arbitrary DNA patterns up to 0.5 micrometers with up to 8,704 pixels.[29] While this idea showed to be successful in 2D and for pure DNA structures, the challenge is to develop experimentally realizable concepts for 3D and for building architectures from nanoscale objects. Tkachenko and coworkers have theoretically utilized chromatic binding to demonstrate a pathway towards achieving a unique hexagonal diamond structure, which can be formed from a minimal mixture of 8 monomers possessing tetrahedral symmetry and a total grouping of 16 unique binding sequences.[79]

The future realization of fully designed 3D architectures may use a chromatic binding strategy through the 'material voxel' platform (Fig. 5D), whereby DNA-frames integrate nano-objects and provide them with both polychromatic and anisotropic bonds.[5c, 21a] Indeed, while

hybridization of origami[5d] allows for the building of ordered 3D frameworks, a multiple hybridization system based on bond specificity opens the possibility of introducing sequence-specific, colored binding at the vertices or faces of selected topologies. Recent studies have used binding specificity in a lattice of DNA origami octahedra to build planar organization of particles.[81] [82]. These groups used different binding specificities at different octahedra vertices, and given the permutation space of 4^n sequences at a given *n* sequence length, a large library of sequence binding 'colors' is available. Thus, such an approach is a promising strategy for prescribing larger scale nanomaterial systems since it allows one to introduce the desired material nano-objects and encode the connectivity between them for achieving a targeted structure. Though this binding color library is theoretically large, DNA assembly requires that binding sets not possess sequence overlaps to reduce off-target binding, and secondary structure formations must be minimized. Additionally, the spread of bond energies might present a challenge for optimizing an assembly pathway, and this aspect should be accounted in potential designs. Furthermore, though vertex-vertex binding minimizes the potential for mis-aligned frames, face-face binding between nanoscale topologies must account for such possibilities.

Zhiwei et al. approached these possibilities by introducing polychromatic binding sets for individual inter-origami interactions between hollow cuboid structures (termed DNA nano-chambers) [21a], shown in **Figure 6G**. These composite bonds allow a much higher degree of encoding through the use of multiple DNA strands in a single neighbor binding interaction. Additionally, they permit tuning the bonds characteristics and orientation of linked origami. For example, two different binding interactions, each held together through 8 bonds, may consist of the same 4 sequence binding set, but permuted differently. This binding fingerprint, acting as a 'permutation of permutations', enables a high degree of bond encoding, through multiple sequences rather than one. This allows for increased binding complexity from a small sequence set, as well as control over the mutual orientation and alignment of encoded components. This control was shown through the construction of 1D, 2D, and 3D systems, with the capability of chiral particle constructs assembled through specific DNA binding sequence combinations on individual faces. Importantly, this study demonstrated that to support the growth of different structures, different numbers of bonds were needed based on both the binding direction and overall dimensionality of growth. For example, in **Figure 6G(i)**, 1D assemblies grow through a 4-bond interaction in the z direction, while in **6G(iii)**, 3D assembly is mediated by 16 bonds in the *z* direction.

To consider such assembly processes more generally, however, the energy landscape of anisotropic structure formation is also a major consideration when viewing yields and defects, with works suggesting a functional upper limit to the number of unique particles used in arbitrary structure synthesis from equilibrium interactions.[83] Thus, the relationship between desired structural complexity and the chromatic interactions utilized to connect the topological building blocks becomes increasingly important as research groups rapidly expand the capability to produce defined structure at the nanoscale.[84] Additionally, the rapid improvement[4g, 62a, 65, 85] in our ability to generate nanoparticles with specifically prescribed spatial anisotropic and colored bonds opens exciting opportunities for their use in assembly of complex 3D architectures.

4. Summary and outlook

Traditional views of building or imposing order on nanoparticle assemblies are inherently limited by an inability to access non-arbitrary structure and pattern formation. Work over the past

two decades has demonstrated the power of programmable assembly, introduced by DNA, for directing an organization of materials at the nanoscales. More recent strides have proven that chromatic binding, in combination with valence-defined and coordinative material binding, can enable a new generation of materials synthesis. In this regime, the boundary between particle and its defining structural frame becomes less clear; a monomer scaffold, or DNA material voxel in this instance, must possess binding specificities for neighboring scaffolds as well as specificity for material binding. The material voxel acts both as a minimal scaffold component and a designable structure itself.

For the first time in nanoparticle crystallization, we can begin to distinguish material form from function by using both defined binding topology and binding specificity to separate particles from strictly energetically-favorable geometric packing. As opposed to macroscale systems, where more straightforward engineering can modify a given material without affecting its inherent properties, a bare material's form and function are inexorably linked at the nanoscale. This requires a rethinking of current assembly methods and the addition of a forward-looking component to nanoscale, topological interaction—specificity, otherwise called chromatic binding.

To gain full access to three-dimensional structure without the need for a fully-prescribed materials, we further propose an interplay between two classes of chromatic binding—those defining interactions between scaffolds and those defining each scaffold's specific connection to a selected particle or material. At the nanoscale, where the number of unique components and binding regimes not only is a technical issue to model and produce but directly contributes to entropic considerations, addressable structure can not only be a matter of fully defining a 3D space. A material voxel, while offering the ability to fully define a volume, importantly offers the capability to minimize overall system complexity to achieve a desired outcome. Control over 3D lattice morphology and particle placement within that structure offers an exciting path forward to moving theory into actual practice. Addressability within 3D space allows one to break from traditional synthesis schemes, which often attempt to expand atomic analogues into larger scales, in order to explore the creation of novel and impactful 3D materials architectures.

Realizing the fabrication of functional devices from these architectures must consider new assembly questions focused on how chromatic binding is incorporated into a desired assembly. Though a DNA binding sequence set can be obtained through inverse design considerations, development of these materials requires further experimentation to see how sequence selection and redundancy affect resulting crystal dimensions and geometry as well as defect incorporation. As discussed, while a fully-prescribed 3D space may not be required, a minimal set of components may not provide the desired material growth or function. In practice, design rules for chromatic materials organization must be explored and defined as materials are synthesized with this new assembly pathway.

As soon as we can demonstrate control over creating complex nanoparticle organizations, there will be increasing interest to utilize these highly engineered materials for a variety of applications. This need requires the establishment of methods that convert these organizations into robust forms. Several approaches were recently introduced that show the ability to template DNA with inorganic materials and preserve a complex 3D organization of DNA nanostructures and nanoparticle components,[25a, 25b, 81a, 86] enabling a creation of functional and robust nanomaterials using DNA-assembly methods.[81a, 87] Thus, in coupling the enormous power of DNA to organize nanoscale objects via designed bottom-up processes with recent advances in inorganic templating, DNA-based assembly offers vast potential to establish a designer platform for fabricating and manufacturing complexly prescribed nanomaterials.

Works Cited

[1] a.) M. Kadic, G. W. Milton, M. van Hecke, M. Wegener, *Nature Reviews Physics* **2019**, *1*, 198-210; b.) K. Roy, A. Jaiswal, P. Panda, *Nature* **2019**, *575*, 607-617; c.) J. A. Liddle, G. M. Gallatin, *ACS Nano* **2016**, *10*, 2995-3014; d.) M. Kjaergaard, M. E. Schwartz, J. Braumüller, P. Krantz, J. I.-J. Wang, S. Gustavsson, W. D. Oliver, *Annual Review of Condensed Matter Physics* **2020**, *11*, 369-395; e.) J. E. Melzer, E. McLeod, *Nanophotonics* **2020**, *9*, 1373-1390; f.) H. An, M. A. Ehsan, Z. Zhou, F. Shen, Y. Yi, *Integration* **2019**, *65*, 273-281; g.) D. Rosenberg, D. Kim, R. Das, D. Yost, S. Gustavsson, D. Hover, P. Krantz, A. Melville, L. Racz, G. O. Samach, S. J. Weber, F. Yan, J. L. Yoder, A. J. Kerman, W. D. Oliver, *npj Quantum Information* **2017**, *3*, 42; h.) J. U. Surjadi, L. Gao, H. Du, X. Li, X. Xiong, N. X. Fang, Y. Lu, *Adv. Eng. Mater.* **2019**, *21*, 1800864; i.) M. M. Shulaker, G. Hills, R. S. Park, R. T. Howe, K. Saraswat, H. S. P. Wong, S. Mitra, *Nature* **2017**, *547*, 74-78.

[2] a.) G. M. Whitesides, B. Grzybowski, *Science* **2002**, *295*, 2418-2421; b.) M. A. Boles, M. Engel, D. V. Talapin, *Chemical Reviews* **2016**, *116*, 11220-11289.

[3] a.) K. W. Tan, U. Wiesner, *Macromolecules* **2019**, *52*, 395-409; b.) A. Klinkova, R. M. Choueiri, E. Kumacheva, *Chem. Soc. Rev.* **2014**, *43*, 3976-3991; c.) C. Yuan, W. Ji, R. Xing, J. Li, E. Gazit, X. Yan, *Nature Reviews Chemistry* **2019**, *3*, 567-588; d.) T. R. Cook, Y.-R. Zheng, P. J. Stang, *Chem. Rev.* **2013**, *113*, 734-777; e.) E. J. Robertson, A. Battigelli, C. Proulx, R. V. Mannige, T. K. Haxton, L. Yun, S. Whitelam, R. N. Zuckermann, *Acc. Chem. Res.* **2016**, *49*, 379-389; f.) J. S. Kahn, B. Minevich, O. Gang, *Curr. Opin. Biotechnol.* **2020**, *63*, 142-150; g.) F. Hong, F. Zhang, Y. Liu, H. Yan, *Chem. Rev.* **2017**, *117*, 12584-12640; h.) A. Heuer-Jungemann, T. Liedl, *Trends in Chemistry* **2019**, *1*, 799-814.

[4] a.) H. Xing, Z. Wang, Z. Xu, N. Y. Wong, Y. Xiang, G. L. Liu, Y. Lu, *ACS Nano* **2012**, *6*, 802-809; b.) Y. Tian, T. Wang, W. Liu, H. L. Xin, H. Li, Y. Ke, W. M. Shih, O. Gang, *Nat Nano* **2015**, *10*, 637-644; c.) J. A. Fan, C. Wu, K. Bao, J. Bao, R. Bardhan, N. J. Halas, V. N. Manoharan, P. Nordlander, G. Shvets, F. Capasso, *Science* **2010**, *328*, 1135; d.) Z. Lu, Y. Yin, *Chem. Soc. Rev.* **2012**, *41*, 6874-6887; e.) C. Yi, H. Liu, S. Zhang, Y. Yang, Y. Zhang, Z. Lu, E. Kumacheva, Z. Nie, *Science* **2020**, *369*, 1369-1374; f.) H. Zhang, M. Li, K. Wang, Y. Tian, J.-S. Chen, K. T. Fountaine, D. DiMarzio, M. Liu, M. Cotlet, O. Gang, *ACS Nano* **2020**, *14*, 1369-1378; g.) S. Sun, S. Yang, H. L. Xin, D. Nykypanchuk, M. Liu, H. Zhang, O. Gang, *Nature Communications* **2020**, *11*, 2279; h.) T. Zhang, T. Liedl, *Nanomaterials* **2019**, *9*, 339.

[5] a.) N. C. Seeman, O. Gang, *Mrs Bulletin* **2017**, *42*, 904-912; b.) R. J. Macfarlane, B. Lee, M. R. Jones, N. Harris, G. C. Schatz, C. A. Mirkin, *Science* **2011**, *334*, 204; c.) Y. Tian, J. R. Lhermitte, L. Bai, T. Vo, H. L. Xin, H. Li, R. Li, M. Fukuto, K. G. Yager, J. S. Kahn, Y. Xiong, B. Minevich, S. K. Kumar, O. Gang, *Nature Materials* **2020**, *19*, 789-796; d.) T. Zhang, C. Hartl, K. Frank, A. Heuer-Jungemann, S. Fischer, P. C. Nickels, B. Nickel, T. Liedl, *Adv. Mater.* **2018**, *30*, 1800273; e.) D. Nykypanchuk, M. M. Maye, D. van der Lelie, O. Gang, *Nature* **2008**, *451*, 549-552; f.) P. Wang, J.-H. Huh, H. Park, D. Yang, Y. Zhang, Y. Zhang, J. Lee, S. Lee, Y. Ke, *Nano Letters* **2020**, *20*, 8926-8932; g.) W. Liu, J. Halverson, Y. Tian, A.

V. Tkachenko, O. Gang, *Nature Chemistry* **2016**, *8*, 867; h.) A. M. Mohammed, P. Šulc, J. Zenk, R. Schulman, *Nature Nanotechnology* **2017**, *12*, 312-316; i.) S. Srivastava, D. Nykypanchuk, M. Fukuto, J. D. Halverson, A. V. Tkachenko, K. G. Yager, O. Gang, *Journal of the American Chemical Society* **2014**, *136*, 8323-8332.

[6] a.) S. Xin, Y. You, S. Wang, H.-C. Gao, Y.-X. Yin, Y.-G. Guo, *ACS Energy Letters* **2017**, *2*, 1385-1394; b.) J. Liu, P. Kopold, P. A. van Aken, J. Maier, Y. Yu, *Angew. Chem. Int. Ed.* **2015**, *54*, 9632-9636; c.) M. H. Ahmadi, M. Ghazvini, M. Alhuyi Nazari, M. A. Ahmadi, F. Pourfayaz, G. Lorenzini, T. Ming, *International Journal of Energy Research* **2019**, *43*, 1387-1410.

[7] a.) A. D. Kent, D. C. Worledge, *Nature Nanotechnology* **2015**, *10*, 187-191; b.) J. Jena, B. Göbel, T. Ma, V. Kumar, R. Saha, I. Mertig, C. Felser, S. S. P. Parkin, *Nature Communications* **2020**, *11*, 1115; c.) K. Chen, J. Zhu, F. Bošković, U. F. Keyser, *Nano Lett.* **2020**, *20*, 3754-3760; d.) G. M. Church, Y. Gao, S. Kosuri, *Science* **2012**, *337*, 1628; e.) J. H. Choi, H. Wang, S. J. Oh, T. Paik, P. S. Jo, J. Sung, X. C. Ye, T. S. Zhao, B. T. Diroll, C. B. Murray, C. R. Kagan, *Science* **2016**, *352*, 205-208.

[8] a.) A. Cecconello, J. S. Kahn, C.-H. Lu, L. Khosravi Khorashad, A. O. Govorov, I. Willner, *Journal of the American Chemical Society* **2016**, *138*, 9895-9901; b.) D.-P. Song, S. Shahin, W. Xie, S. Mehravar, X. Liu, C. Li, R. A. Norwood, J.-H. Lee, J. J. Watkins, *Macromolecules* **2016**, *49*, 5068-5075; c.) H. M. Xiong, M. Y. Sfeir, O. Gang, *Nano Lett.* **2010**, *10*, 4456-4462; d.) A. Kuzyk, R. Schreiber, Z. Y. Fan, G. Pardatscher, E. M. Roller, A. Hogele, F. C. Simmel, A. O. Govorov, T. Liedl, *Nature* **2012**, *483*, 311-314; e.) F. Nicoli, T. Zhang, K. Hübner, B. Jin, F. Selbach, G. Acuna, C. Argyropoulos, T. Liedl, M. Pilo-Pais, *Small* **2019**, *15*, 1804418; f.) D. Sun, Y. Tian, Y. Zhang, Z. Xu, M. Y. Sfeir, M. Cotlet, O. Gang, *ACS Nano* **2015**, *9*, 5657-5665.

[9] a.) C. M. Niemeyer, J. Koehler, C. Wuerdemann, *ChemBioChem* **2002**, 242-245; b.) M. Vázquez-González, C. Wang, I. Willner, *Nature Catalysis* **2020**, *3*, 256-273; c.) W.-H. Chen, M. Vázquez-González, A. Zoabi, R. Abu-Reziq, I. Willner, *Nature Catalysis* **2018**, *1*, 689-695; d.) Y. Yamada, C.-K. Tsung, W. Huang, Z. Huo, S. E. Habas, T. Soejima, C. E. Aliaga, G. A. Somorjai, P. Yang, *Nature Chemistry* **2011**, *3*, 372.

[10] a.) M. R. Jones, R. J. Macfarlane, B. Lee, J. Zhang, K. L. Young, A. J. Senesi, C. A. Mirkin, *Nature Materials* **2010**, *9*, 913; b.) S. C. Glotzer, M. J. Solomon, *Nature Mater.* **2007**, *6*, 557-562.

[11] a.) N. C. Seeman, *Journal of Theoretical Biology* **1982**, *99*, 237-247; b.) P. F. Damasceno, M. Engel, S. C. Glotzer, *Science* **2012**, *337*, 453-457.

[12] a.) A. P. Alivisatos, K. P. Johnsson, X. G. Peng, T. E. Wilson, C. J. Loweth, M. P. Bruchez, P. G. Schultz, *Nature* **1996**, *382*, 609-611; b.) C. A. Mirkin, R. L. Letsinger, R. C. Mucic, J. J. Storhoff, *Nature* **1996**, *382*, 607-609.

[13] a.) M. R. Jones, N. C. Seeman, C. A. Mirkin, *Science* **2015**, *347*, 1260901; b.) E. Benson, A. Mohammed, J. Gardell, S. Masich, E. Czeizler, P. Orponen, B. Högberg, *Nature* **2015**, *523*, 441-444; c.) D. S. Hopkins, D. Pekker, P. M. Goldbart, A. Bezryadin, *Science* **2005**, *308*, 1762-1765; d.) E. Braun , K. Keren, *Advances in Physics* **2004**, *53*, 441-496; e.) E. Stulz, *Chemistry–A European Journal* **2012**, *18*, 4456-4469.

[14] a.) E. Winfree, F. Liu, L. A. Wenzler, N. C. Seeman, *Nature* **1998**, *394*, 539-544; b.) C. Mao, W. Sun, N. C. Seeman, *Journal of the American Chemical Society* **1999**, *121*, 5437-

5443; c.) P. W. K. Rothemund, *Nature* **2006**, *440*, 297-302; d.) M. Shekhirev, E. Sutter, P. Sutter, *Adv. Funct. Mater.* **2019**, *29*, 1806924.

[15] a.) H. Dietz, S. M. Douglas, W. M. Shih, *Science* **2009**, *325*, 725-730; b.) J. Zheng, J. J. Birktoft, Y. Chen, T. Wang, R. Sha, P. E. Constantinou, S. L. Ginell, C. Mao, N. C. Seeman, *Nature* **2009**, *461*, 74-77; c.) D. Han, S. Pal, J. Nangreave, Z. Deng, Y. Liu, H. Yan, *Science* **2011**, *332*, 342-346; d.) F. Zhang, S. Jiang, S. Wu, Y. Li, C. Mao, Y. Liu, H. Yan, *Nat Nanotechnol.* **2015**, *10*, 779-784; e.) N. N. Ma, B. Minevich, J. L. Liu, M. Ji, Y. Tian, O. Gang, *Top. Curr. Chem.* **2020**, *378*, 157-190; f.) F. Zhang, C. R. Simmons, J. Gates, Y. Liu, H. Yan, *Angew. Chem. Int. Ed.* **2018**, *57*, 12504-12507; g.) J. Chen, N. C. Seeman, *Nature* **1991**, *350*, 631-633; h.) S. M. Douglas, H. Dietz, T. Liedl, B. Hogberg, F. Graf, W. M. Shih, *Nature* **2009**, *459*, 414-418; i.) M. Matthies, N. P. Agarwal, E. Poppleton, F. M. Joshi, P. Šulc, T. L. Schmidt, *ACS Nano* **2019**, *13*, 1839-1848.

[16] E. Sutter, B. Zhang, S. Sutter, P. Sutter, *Nanoscale* **2019**, *11*, 34-44.

[17] a.) S. Y. Park, A. K. R. Lytton-Jean, B. Lee, S. Weigand, G. C. Schatz, C. A. Mirkin, *Nature* **2008**, *451*, 553-556; b.) H. M. Xiong, D. van der Lelie, O. Gang, *Phys. Rev. Lett.* **2009**, *102*, 015504; c.) M. R. Jones, R. J. Macfarlane, B. Lee, J. Zhang, K. L. Young, A. J. Senesi, C. A. Mirkin, *Nature Materials* **2010**, *9*, 913-917; d.) D. J. Lewis, L. Z. Zornberg, D. J. D. Carter, R. J. Macfarlane, *Nature Materials* **2020**, *19*, 719-724; e.) Y. Zhang, S. Pal, B. Srinivasan, T. Vo, S. Kumar, O. Gang, *Nature Materials* **2015**, *14*, 840-847.

[18] A. F. De Fazio, A. H. El-Sagheer, J. S. Kahn, I. Nandhakumar, M. R. Burton, T. Brown, O. L. Muskens, O. Gang, A. G. Kanaras, *ACS Nano* **2019**, *13*, 5771-5777.

[19] a.) Z. Lin, Y. Xiong, S. Xiang, O. Gang, *Journal of the American Chemical Society* **2019**, *141*, 6797-6801; b.) J. Zhang, Z. Di, H. Yan, Y. Zhao, L. Li, *Nano Letters* **2021**, *21*, 2793-2799; c.) S. Srivastava, M. Fukuto, O. Gang, *Soft Matter* **2018**, *14*, 3929-3934; d.) A. L. Stadler, D. Sun, M. M. Maye, D. van der Lelie, O. Gang, *ACS Nano* **2011**, *5*, 2467-2474.

[20] a.) J. Zheng, P. E. Constantinou, C. Micheel, A. P. Alivisatos, R. A. Kiehl, N. C. Seeman, *Nano Lett.* **2006**, *6*, 1502-1504; b.) H. Li, S. H. Park, J. H. Reif, T. H. LaBean, H. Yan, *Journal of the American Chemical Society* **2004**, *126*, 418-419; c.) J. Zhang, Y. Liu, Y. Ke, H. Yan, *Nano Letters* **2006**, *6*, 248-251.

[21] a.) Z. Lin, H. Emamy, B. Minevich, Y. Xiong, S. Xiang, S. Kumar, Y. Ke, O. Gang, *Journal of the American Chemical Society* **2020**, *142*, 17531-17542; b.) Y. Tian, Y. Zhang, T. Wang, H. L. Xin, H. Li, O. Gang, *Nature Materials* **2016**, *15*, 654; c.) C. Tian, M. A. L. Cordeiro, J. Lhermitte, H. L. Xin, L. Shani, M. Liu, C. Ma, Y. Yeshurun, D. DiMarzio, O. Gang, *ACS Nano* **2017**, *11*, 7036-7048; d.) R. Schreiber, J. Do, E.-M. Roller, T. Zhang, V. J. Schüller, P. C. Nickels, J. Feldmann, T. Liedl, *Nature Nanotechnology* **2014**, *9*, 74-78.

[22] Y. Zhang, F. Lu, K. G. Yager, D. van der Lelie, O. Gang, *Nature Nanotechnology* **2013**, *8*, 865.

[23] W. Liu, M. Tagawa, H. L. Xin, T. Wang, H. Emamy, H. Li, K. G. Yager, F. W. Starr, A. V. Tkachenko, O. Gang, *Science* **2016**, *351*, 582 LP-586.

[24] a.) W. Liu, H. Zhong, R. Wang, N. C. Seeman, *Angew. Chem. Int. Ed.* **2011**, *50*, 264-267; b.) F. Hong, S. Jiang, X. Lan, R. P. Narayanan, P. Šulc, F. Zhang, Y. Liu, H. Yan, *Journal of the American Chemical Society* **2018**, *140*, 14670-14676; c.) C. R. Simmons, F. Zhang, T. MacCulloch, N. Fahmi, N. Stephanopoulos, Y. Liu, N. C. Seeman, H. Yan, *Journal of the American Chemical Society* **2017**, *139*, 11254-11260; d.) Y. Hao, M. Kristiansen, R. Sha, J.

J. Birktoft, C. Hernandez, C. Mao, N. C. Seeman, *Nature Chemistry* **2017**, *9*, 824-827; e.) C. R. Simmons, T. MacCulloch, F. Zhang, Y. Liu, N. Stephanopoulos, H. Yan, *Angewandte Chemie International Edition* **2020**, *59*, 18619-18626; f.) Z. Li, L. Liu, M. Zheng, J. Zhao, N. C. Seeman, C. Mao, *Journal of the American Chemical Society* **2019**, *141*, 15850-15855.

[25] a.) L. Nguyen, M. Döblinger, T. Liedl, A. Heuer-Jungemann, *Angew. Chem. Int. Ed.* **2019**, *58*, 912-916; b.) X. Liu, F. Zhang, X. Jing, M. Pan, P. Liu, W. Li, B. Zhu, J. Li, H. Chen, L. Wang, J. Lin, Y. Liu, D. Zhao, H. Yan, C. Fan, *Nature* **2018**, *559*, 593-598; c.) S. Jia, J. Wang, M. Xie, J. Sun, H. Liu, Y. Zhang, J. Chao, J. Li, L. Wang, J. Lin, K. V. Gothelf, C. Fan, *Nature Communications* **2019**, *10*, 5597; d.) K. Keren, R. S. Berman, E. Braun, *Nano Lett.* **2004**, *4*, 323-326; e.) F. Zhou, W. Sun, K. B. Ricardo, D. Wang, J. Shen, P. Yin, H. Liu, *ACS Nano* **2016**, *10*, 3069-3077.

[26] F. Lu, K. G. Yager, Y. Zhang, H. Xin, O. Gang, *Nature Communications* **2015**, *6*, 6912.

[27] Y. Wang, Y. Wang, D. R. Breed, V. N. Manoharan, L. Feng, A. D. Hollingsworth, M. Weck, D. J. Pine, *Nature* **2012**, *491*, 51-56.

[28] Y. He, Y. Tian, A. E. Ribbe, C. Mao, *Journal of the American Chemical Society* **2006**, *128*, 15978-15979.

[29] G. Tikhomirov, P. Petersen, L. Qian, *Nature* **2017**, *552*, 67-71.

[30] L. Liu, Z. Li, Y. Li, C. Mao, *Journal of the American Chemical Society* **2019**, *141*, 4248-4251.

[31] a.) E. Shevchenko, D. Talapin, A. Kornowski, F. Wiekhorst, J. Kötzler, M. Haase, A. Rogach, H. Weller, *Adv. Mater.* **2002**, *14*, 287-290; b.) D. V. Talapin, E. V. Shevchenko, M. I. Bodnarchuk, X. C. Ye, J. Chen, C. B. Murray, *Nature* **2009**, *461*, 964-967.

[32] H. Zhang, S. Nayak, W. Wang, S. Mallapragada, D. Vaknin, *Langmuir* **2017**, *33*, 12227-12234.

[33] a.) C. R. Laramy, M. N. O'Brien, C. A. Mirkin, *Nature Reviews Materials* **2019**, *4*, 201-224; b.) S. J. Tan, J. S. Kahn, T. L. Derrien, M. J. Campolongo, M. Zhao, D.-M. Smilgies, D. Luo, *Angew. Chem. Int. Ed.* **2014**, *53*, 1316-1319; c.) R. Ni, A. P. Gantapara, J. de Graaf, R. van Roij, M. Dijkstra, *Soft Matter* **2012**, *8*, 8826-8834; d.) B. Srinivasan, T. Vo, Y. Zhang, O. Gang, S. Kumar, V. Venkatasubramanian, *Proceedings of the National Academy of Sciences* **2013**, *110*, 18431.

[34] R. J. Macfarlane, M. R. Jones, A. J. Senesi, K. L. Young, B. Lee, J. Wu, C. A. Mirkin, *Angew. Chem. Int. Ed.* **2010**, *49*, 4589-4592.

[35] a.) A. V. Tkachenko, *Phys. Rev. Lett.* **2002**, *89*, 148303; b.) P. L. Biancaniello, A. J. Kim, J. C. Crocker, *Phys. Rev. Lett.* **2005**, *94*, 058302; c.) N. A. Licata, A. V. Tkachenko, *Physical Review E* **2006**, *74*, 041408; d.) M. E. Leunissen, D. Frenkel, *The Journal of Chemical Physics* **2011**, *134*, 084702; e.) T. I. N. G. Li, R. Sknepnek, R. J. Macfarlane, C. A. Mirkin, M. Olvera de la Cruz, *Nano Lett.* **2012**, *12*, 2509-2514; f.) F. J. Martinez-Veracoechea, B. M. Mladek, A. V. Tkachenko, D. Frenkel, *Phys. Rev. Lett.* **2011**, *107*, 045902; g.) B. M. Mladek, J. Fornleitner, F. J. Martinez-Veracoechea, A. Dawid, D. Frenkel, *Soft Matter* **2013**, *9*, 7342-7355.

[36] W. Liu, N. A. Mahynski, O. Gang, A. Z. Panagiotopoulos, S. K. Kumar, *ACS Nano* **2017**, *11*, 4950-4959.

[37] a.) F. Sciortino, Y. Zhang, O. Gang, S. K. Kumar, *ACS Nano* **2020**, *14*, 5628-5635; b.) M. Song, Y. Ding, H. Zerze, M. A. Snyder, J. Mittal, *Langmuir* **2018**, *34*, 991-998; c.) C.

Knorowski, A. Travesset, *Soft Matter* **2012**, *8*, 12053-12059; d.) E. Pretti, R. Mao, J. Mittal, *Molecular Simulation* **2019**, *45*, 1203-1210; e.) S. Pan, N. Boon, M. Olvera de la Cruz, *ACS Nano* **2016**, *10*, 9948-9956; f.) M. Girard, J. A. Millan, M. Olvera de la Cruz, *Annual Review of Materials Research* **2017**, *47*, 33-49; g.) J. O'Leary, R. Mao, E. J. Pretti, J. A. Paulson, J. Mittal, A. Mesbah, *Soft Matter* **2021**, *17*, 989-999; h.) M. M. Maye, D. Nykypanchuk, D. van der Lelie, O. Gang, *Small* **2007**, *3*, 1678-1682; i.) M. M. Maye, D. Nykypanchuk, D. van der Lelie, O. Gang, *Journal of the American Chemical Society* **2006**, *128*, 14020-14021; j.) D. Nykypanchuk, M. M. Maye, D. van der Lelie, O. Gang, *Langmuir* **2007**, *23*, 6305-6314; k.) E. Pretti, H. Zerze, M. Song, Y. Ding, N. A. Mahynski, H. W. Hatch, V. K. Shen, J. Mittal, *Soft Matter* **2018**, *14*, 6303-6312.

[38] a.) V. N. Manoharan, M. T. Elsesser, D. J. Pine, *Science* **2003**, *301*, 483-487; b.) G. N. Meng, N. Arkus, M. P. Brenner, V. N. Manoharan, *Science* **2010**, *327*, 560-563; c.) A. Travesset, *Phys. Rev. Lett.* **2017**, *119,* 115701.

[39] S. Srivastava, D. Nykypanchuk, M. M. Maye, A. V. Tkachenko, O. Gang, *Soft Matter* **2013**, *9*, 10452-10457.

[40] a.) E. V. Shevchenko, D. V. Talapin, N. A. Kotov, S. O'Brien, C. B. Murray, *Nature* **2006**, *439*, 55-59; b.) D. V. Talapin, J.-S. Lee, M. V. Kovalenko, E. V. Shevchenko, *Chem. Rev.* **2010**, *110*, 389-458; c.) N. Horst, A. Travesset, *J. Chem. Phys.* **2016**, *144*, 014502.

[41] T. Vo, V. Venkatasubramanian, S. Kumar, B. Srinivasan, S. Pal, Y. G. Zhang, O. Gang, *Proceedings of the National Academy of Sciences of the United States of America* **2015**, *112*, 4982-4987.

[42] O. Gang, A. V. Tkachenko, *MRS Bull.* **2016**, *41*, 381-387.

[43] a.) S. E. Seo, M. Girard, M. O. de la Cruz, C. A. Mirkin, *ACS Central Science* **2019**, *5*, 186-191; b.) J. A. Mason, C. R. Laramy, C.-T. Lai, M. N. O'Brien, Q.-Y. Lin, V. P. Dravid, G. C. Schatz, C. A. Mirkin, *Journal of the American Chemical Society* **2016**, *138*, 8722-8725; c.) S. Pal, Y. Zhang, S. K. Kumar, O. Gang, *Journal of the American Chemical Society* **2015**, *137*, 4030-4033.

[44] a.) Y. Wang, Y. Wang, X. Zheng, É. Ducrot, J. S. Yodh, M. Weck, D. J. Pine, *Nature Communications* **2015**, *6*, 7253; b.) D. Sun, O. Gang, *Journal of the American Chemical Society* **2011**, *133*, 5252-5254.

[45] D. V. Talapin, E. V. Shevchenko, M. I. Bodnarchuk, X. Ye, J. Chen, C. B. Murray, *Nature* **2009**, *461*, 964.

[46] I. Coropceanu, M. A. Boles, D. V. Talapin, *Journal of the American Chemical Society* **2019**, *141*, 5728-5740.

[47] E. Auyeung, T. I. N. G. Li, A. J. Senesi, A. L. Schmucker, B. C. Pals, M. O. de la Cruz, C. A. Mirkin, *Nature* **2014**, *505*, 73-77.

[48] a.) M. T. Casey, R. T. Scarlett, W. Benjamin Rogers, I. Jenkins, T. Sinno, J. C. Crocker, *Nature Communications* **2012**, *3*, 1209; b.) S. Ren, Y. Sun, F. Zhang, A. Travesset, C.-Z. Wang, K.-M. Ho, *ACS Nano* **2020**, *14*, 6795-6802.

[49] a.) M. N. O'Brien, M. R. Jones, B. Lee, C. A. Mirkin, *Nature Materials* **2015**, *14*, 833; b.) M. N. O'Brien, M. Girard, H. X. Lin, J. A. Millan, M. O. de la Cruz, B. Lee, C. A. Mirkin, *Proceedings of the National Academy of Sciences of the United States of America* **2016**, *113*, 10485-10490; c.) M. R. Jones, R. J. Macfarlane, A. E. Prigodich, P. C. Patel, C. A.

Mirkin, *Journal of the American Chemical Society* **2011**, *133*, 18865-18869; d.) C. Knorowski, A. Travesset, *Journal of the American Chemical Society* **2014**, *136*, 653-659.

[50] a.) L. Rossi, S. Sacanna, W. T. M. Irvine, P. M. Chaikin, D. J. Pine, A. P. Philipse, *Soft Matter* **2011**, *7*, 4139-4142; b.) R. D. Batten, F. H. Stillinger, S. Torquato, *Physical Review E* **2010**, *81*, 061105; c.) H. Chan, A. Demortiere, L. Vukovic, P. Kral, C. Petit, *Acs Nano* **2012**, *6*, 4203-4213; d.) K. L. Gurunatha, S. Marvi, G. Arya, A. R. Tao, *Nano Lett.* **2015**, *15*, 7377-7382; e.) M. R. Khadilkar, U. Agarwal, F. A. Escobedo, *Soft Matter* **2013**, *9*, 11557-11567; f.) R. P. Li, K. F. Bian, Y. X. Wang, H. W. Xu, J. A. Hollingsworth, T. Hanrath, J. Y. Fang, Z. W. Wang, *Nano Lett.* **2015**, *15*, 6254-6260; g.) G. Soligno, M. Dijkstra, R. van Roij, *Phys. Rev. Lett.* **2016**, *116*, 258001; h.) Y. Zhang, F. Lu, D. v. d. Lelie, O. Gang, *Phy. Rev. Lett.* **2011**, *107*, 135701; i.) E. Nakouzi, J. A. Soltis, B. A. Legg, G. K. Schenter, X. Zhang, T. R. Graham, K. M. Rosso, L. M. Anovitz, J. J. De Yoreo, J. Chun, *Acs Nano* **2018**, *12*, 10114-10122; j.) D. Wang, M. Hermes, R. Kotni, Y. T. Wu, N. Tasios, Y. Liu, B. de Nijs, E. B. van der Wee, C. B. Murray, M. Dijkstra, A. van Blaaderen, *Nature Communications* **2018**, *9*, 2228.

[51] F. Lu, T. Vo, Y. Zhang, A. Frenkel, K. G. Yager, S. Kumar, O. Gang, *Science Advances* **2019**, *5*, eaaw2399.

[52] H. Lin, S. Lee, L. Sun, M. Spellings, M. Engel, S. C. Glotzer, C. A. Mirkin, *Science* **2017**, *355*, 931.

[53] M. Dijkstra, D. Frenkel, J. P. Hansen, *The Journal of Chemical Physics* **1994**, *101*, 3179-3189.

[54] S. Vial, D. Nykypanchuk, K. G. Yager, A. V. Tkachenko, O. Gang, *ACS Nano* **2013**, *7*, 5437-5445.

[55] a.) G. van Anders, N. K. Ahmed, R. Smith, M. Engel, S. C. Glotzer, *Acs Nano* **2014**, *8*, 931-940; b.) F. Romano, E. Sanz, F. Sciortino, *J. Chem. Phys.* **2010**, *132*, 184501; c.) J. Russo, P. Tartaglia, F. Sciortino, *Soft Matter* **2010**, *6*, 4229-4236.

[56] a.) Q. Chen, S. C. Bae, S. Granick, *Nature* **2012**, *469*, 381-384; b.) M. Y. Ben Zion, X. J. He, C. C. Maass, R. J. Sha, N. C. Seeman, P. M. Chaikin, *Science* **2017**, *358*, 633-+; c.) Y. Wang, A. D. Hollingsworth, S. K. Yang, S. Patel, D. J. Pine, M. Weck, *Journal of the American Chemical Society* **2013**, *135*, 14064–14067.

[57] a.) Z. Zhang, S. C. Glotzer, *Nano Lett.* **2004**, *4*, 1407-1413; b.) T. Vissers, Z. Preisler, F. Smallenburg, M. Dijkstra, F. Sciortino, *The Journal of Chemical Physics* **2013**, *138*, 164505.

[58] S. Ravaine, E. Duguet, *Current Opinion in Colloid & Interface Science* **2017**, *30*, 45-53.

[59] L. Feng, R. Dreyfus, R. Sha, N. C. Seeman, P. M. Chaikin, *Adv. Mater.* **2013**, *25*, 2779-2783.

[60] M. B. Zanjani, I. C. Jenkins, J. C. Crocker, T. Sinno, *ACS Nano* **2016**, *10*, 11280-11289.

[61] M. He, J. P. Gales, É. Ducrot, Z. Gong, G.-R. Yi, S. Sacanna, D. J. Pine, *Nature* **2020**, *585*, 524-529.

[62] a.) T. G. W. Edwardson, K. L. Lau, D. Bousmail, C. J. Serpell, H. F. Sleiman, *Nature Chemistry* **2016**, *8*, 162-170; b.) E. Galati, M. Tebbe, A. Querejeta-Fernández, H. L. Xin, O. Gang, E. B. Zhulina, E. Kumacheva, *ACS Nano* **2017**, *11*, 4995-5002; c.) C. Shen, X. Lan, X. Lu, T. A. Meyer, W. Ni, Y. Ke, Q. Wang, *Journal of the American Chemical Society* **2016**, *138*, 1764-1767.

[63] T. Trinh, C. Liao, V. Toader, M. Barłóg, H. S. Bazzi, J. Li, H. F. Sleiman, *Nature Chemistry* **2017**, *10*, 184.
[64] N. Xie, S. Liu, H. Fang, Y. Yang, K. Quan, J. Li, X. Yang, K. Wang, J. Huang, *ACS Nano* **2019**, *13*, 4174-4182.
[65] Y. Xiong, S. Yang, Y. Tian, A. Michelson, S. Xiang, H. Xin, O. Gang, *ACS Nano* **2020**, *14*, 6823-6833.
[66] G. Chen, K. J. Gibson, D. Liu, H. C. Rees, J.-H. Lee, W. Xia, R. Lin, H. L. Xin, O. Gang, Y. Weizmann, *Nature Materials* **2019**, *18*, 169-174.
[67] J. D. Halverson, A. V. Tkachenko, *Physical Review E* **2013**, *87*, 062310.
[68] a.) S. K. Cha, J. H. Mun, T. Chang, S. Y. Kim, J. Y. Kim, H. M. Jin, J. Y. Lee, J. Shin, K. H. Kim, S. O. Kim, *ACS Nano* **2015**, *9*, 5536-5543; b.) M. S. Onses, L. Wan, X. Liu, N. B. Kiremitler, H. Yılmaz, P. F. Nealey, *ACS Macro Letters* **2015**, *4*, 1356-1361; c.) D.-P. Song, C. Li, N. S. Colella, W. Xie, S. Li, X. Lu, S. Gido, J.-H. Lee, J. J. Watkins, *Journal of the American Chemical Society* **2015**, *137*, 12510-12513.
[69] B. Hatton, L. Mishchenko, S. Davis, K. H. Sandhage, J. Aizenberg, *Proceedings of the National Academy of Sciences* **2010**, *107*, 10354.
[70] a.) R. Boppella, S. T. Kochuveedu, H. Kim, M. J. Jeong, F. Marques Mota, J. H. Park, D. H. Kim, *ACS Applied Materials & Interfaces* **2017**, *9*, 7075-7083; b.) J. Yu, J. Lei, L. Wang, J. Zhang, Y. Liu, *J. Alloys Compd.* **2018**, *769*, 740-757; c.) A. Blanco, E. Chomski, S. Grabtchak, M. Ibisate, S. John, S. W. Leonard, C. Lopez, F. Meseguer, H. Miguez, J. P. Mondia, G. A. Ozin, O. Toader, H. M. van Driel, *Nature* **2000**, *405*, 437.
[71] a.) H. Li, M. Eddaoudi, M. O'Keeffe, O. M. Yaghi, *Nature* **1999**, *402*, 276; b.) O. M. Yaghi, G. Li, H. Li, *Nature* **1995**, *378*, 703; c.) P. Falcaro, R. Ricco, A. Yazdi, I. Imaz, S. Furukawa, D. Maspoch, R. Ameloot, J. D. Evans, C. J. Doonan, *Coord. Chem. Rev.* **2016**, *307*, 237-254; d.) H. K. Chae, D. Y. Siberio-Pérez, J. Kim, Y. Go, M. Eddaoudi, A. J. Matzger, M. O'Keeffe, O. M. Yaghi, *Nature* **2004**, *427*, 523.
[72] a.) L. Jiao, Y. Wang, H.-L. Jiang, Q. Xu, *Adv. Mater.* **2018**, *30*, 1703663; b.) K. Lu, T. Aung, N. Guo, R. Weichselbaum, W. Lin, *Adv. Mater.* **2018**, *30*, 1707634; c.) H. Li, K. Wang, Y. Sun, C. T. Lollar, J. Li, H.-C. Zhou, *Mater. Today* **2018**, *21*, 108-121.
[73] B. Gole, U. Sanyal, R. Banerjee, P. S. Mukherjee, *Inorg. Chem.* **2016**, *55*, 2345-2354.
[74] R. Schreiber, I. Santiago, A. Ardavan, A. J. Turberfield, *ACS Nano* **2016**, *10*, 7303-7306.
[75] a.) Y. He, Y. Chen, H. Liu, A. E. Ribbe, C. Mao, *Journal of the American Chemical Society* **2005**, *127*, 12202-12203; b.) H. Liu, Y. He, A. E. Ribbe, C. Mao, *Biomacromolecules* **2005**, *6*, 2943-2945; c.) F. Liu, R. Sha, N. C. Seeman, *Journal of the American Chemical Society* **1999**, *121*, 917-922; d.) B. Ding, R. Sha, N. C. Seeman, *Journal of the American Chemical Society* **2004**, *126*, 10230-10231.
[76] Y. He, T. Ye, A. E. Ribbe, C. Mao, *Journal of the American Chemical Society* **2011**, *133*, 1742-1744.
[77] P. Wang, S. Gaitanaros, S. Lee, M. Bathe, W. M. Shih, Y. Ke, *Journal of the American Chemical Society* **2016**, *138*, 7733-7740.
[78] L. L. Ong, N. Hanikel, O. K. Yaghi, C. Grun, M. T. Strauss, P. Bron, J. Lai-Kee-Him, F. Schueder, B. Wang, P. Wang, J. Y. Kishi, C. Myhrvold, A. Zhu, R. Jungmann, G. Bellot, Y. Ke, P. Yin, *Nature* **2017**, *552*, 72.
[79] N. Patra, A. V. Tkachenko, *Physical Review E* **2018**, *98*, 032611.

[80] Y. Ke, L. L. Ong, W. M. Shih, P. Yin, *Science* **2012**, *338*, 1177.
[81] a.) L. Shani, A. N. Michelson, B. Minevich, Y. Fleger, M. Stern, A. Shaulov, Y. Yeshurun, O. Gang, *Nature Communications* **2020**, *11*, 5697; b.) M. Ji, J. Liu, L. Dai, L. Wang, Y. Tian, *Journal of the American Chemical Society* **2020**, *142*, 21336-21343.
[82] S.-T. Wang, B. Minevich, J. Liu, H. Zhang, D. Nykypanchuk, J. Byrnes, W. Liu, L. Bershadsky, Q. Liu, T. Wang, G. Ren, O. Gang, *Nature Communications* **in press**.
[83] Z. Zeravcic, V. N. Manoharan, M. P. Brenner, *Proceedings of the National Academy of Sciences* **2014**, *111*, 15918.
[84] a.) H. Jun, X. Wang, W. P. Bricker, S. Jackson, M. Bathe, *bioRxiv* **2020**, DOI: 2020.02.09.940320; b.) H. Jun, T. R. Shepherd, K. Zhang, W. P. Bricker, S. Li, W. Chiu, M. Bathe, *ACS Nano* **2019**, *13*, 2083-2093; c.) H. Jun, X. Wang, W. P. Bricker, M. Bathe, *Nature Communications* **2019**, *10*, 1-9; d.) M. Kube, F. Kohler, E. Feigl, B. Nagel-Yüksel, E. M. Willner, J. J. Funke, T. Gerling, P. Stömmer, M. N. Honemann, T. G. Martin, S. H. W. Scheres, H. Dietz, *Nature Communications* **2020**, *11*, 6229; e.) F. A. S. Engelhardt, F. Praetorius, C. H. Wachauf, G. Brüggenthies, F. Kohler, B. Kick, K. L. Kadletz, P. N. Pham, K. L. Behler, T. Gerling, H. Dietz, *ACS Nano* **2019**, *13*, 5015-5027.
[85] a.) G. Yao, J. Li, Q. Li, X. Chen, X. Liu, F. Wang, Z. Qu, Z. Ge, R. P. Narayanan, D. Williams, H. Pei, X. Zuo, L. Wang, H. Yan, B. L. Feringa, C. Fan, *Nature Materials* **2020**, *19*, 781-788; b.) M. Y. Ben Zion, X. He, C. C. Maass, R. Sha, N. C. Seeman, P. M. Chaikin, *Science* **2017**, *358*, 633-636; c.) Y. Zhang, X. He, R. Zhuo, R. Sha, J. Brujic, N. C. Seeman, P. M. Chaikin, *Proceedings of the National Academy of Sciences* **2018**, *115*, 9086-9091.
[86] a.) A. Michelson, H. Zhang, S. Xiang, O. Gang, *Nano Lett.* **2021**, *21*, 1863-1870; b.) X. Jing, F. Zhang, M. Pan, X. Dai, J. Li, L. Wang, X. Liu, H. Yan, C. Fan, *Nature Protocols* **2019**, *14*, 2416-2436; c.) E. Auyeung, R. J. Macfarlane, C. H. J. Choi, J. I. Cutler, C. A. Mirkin, *Adv. Mater.* **2012**, *24*, 5181-5186.
[87] P. W. Majewski, A. Michelson, M. A. L. Cordeiro, C. Tian, C. Ma, K. Kisslinger, Y. Tian, W. Liu, E. A. Stach, K. G. Yager, O. Gang, *Science Advances* **2021**, *7*, eabf0617.